

Microwave Laboratory Theory and Lab Manuals

S Dutta Gupta

School of Physics, University of Hyderabad
Hyderabad 500046, India

(Lecture Notes for January-May Semester, 2009)

March 22, 2009

Contents

1	Transmission Lines	9
1.1	To study the characteristics of a transmission line, to measure the VSWR for a waveguide section and to measure unknown load impedance	9
1.2	Theoretical background	9
1.2.1	Ideal transmission lines: spatio-temporal dependence of signals	10
1.2.2	Reflection and transmission at a resistive discontinuity	11
1.2.3	Sinusoidal waves on ideal transmission lines	12
1.2.4	The Smith chart for a transmission line	16
1.2.5	Uses of Smith Chart	18
1.2.6	Transmission lines with general forms of distributed impedance (Lossy lines)	21
1.2.7	Transmission line with series and shunt losses	22
1.2.8	Resonant transmission lines	24
1.3	Experiment for VSWR measurement	24
1.3.1	Experimental procedure:	24
1.3.2	Measuring the unknown load impedance:	26
1.3.3	Procedure	26
1.3.4	Estimation of normalized load using Smith chart	27
2	Wave guides	29
2.1	General formulation for guided waves	29
2.1.1	Classification of the waves	31
2.2	Cylindrical waveguiding with various cross sections	31
2.2.1	Metal parallel plate guide	31
2.2.2	TM waves in a rectangular guide	34
3	Directional Coupler	37
3.1	Objectives	37
3.2	Theoretical background	37
3.2.1	N-port waveguide junctions	37
3.2.2	Directional coupler as an example of a four-port junction	38

3.3	Experimental procedure	41
3.4	Conclusions	43
4	Magic Tee	45
4.1	Objectives	45
4.2	Theoretical background	45
4.2.1	<i>E</i> -plane tee	45
4.2.2	<i>H</i> -plane tee	45
4.2.3	Magic tee	45
4.2.4	Isolation	47
4.2.5	Coupling	47
4.3	Experimental procedure	48
5	Klystron	49
5.1	Theoretical background	49
5.1.1	Velocity modulation	51
5.1.2	Power output and efficiency	53
5.2	Apparatus and measurements	55
5.2.1	Experimental setup with VSWR	55
5.2.2	Experimental setup with Oscilloscope:	56
5.2.3	Data collection and analysis	57
5.3	Conclusions	57
6	Gunn Diode	59
6.1	Objectives	59
6.2	Theoretical background	59
6.2.1	The Gunn Effect	59
6.2.2	The Gunn Diode	59
6.2.3	Theory	61
6.3	Experimental Setup	64
6.3.1	Apparatus Required	64
6.3.2	Experimental Procedure	64
6.3.3	Voltage-current characteristics	64
6.3.4	Output power and frequency as function of Gunn bias voltage	65
6.3.5	Mechanical Tuning of Output Power and frequency	65
6.3.6	Square wave modulation through PIN diode	65
7	Horn Antenna	67
7.1	Objectives	67
7.2	Introduction	67
7.3	Experimental setup	68

7.3.1	Apparatus required	68
7.4	Gain	68
7.4.1	Gain of the Horn antenna for E and H planes	68
7.5	Radiation field pattern for E and H planes	70
7.6	3-dB Beam width	71
7.6.1	Acknowledgement	72
8	Dielectric constant of solids	73
8.1	Objective	73
8.2	Theoretical background	73
8.2.1	Graphical and numerical solution of the transcendental Eq.(8.11)	76
8.3	Experimental procedure	76
9	Dielectric Constant of Liquids using Liquid Plunger	81
9.1	Theoretical background	81
9.2	Procedure	82
9.2.1	Lossless case	82
9.2.2	Lossy dielectric	83

Introduction

Procedure for each Lab Experiment

1. The student has to familiarize himself/herself with the necessary theoretical background of the experiment and should be clear about what is to be done and why and how it should be done.
2. He/she has to appear for a viva in order to be allowed to do the experiment.
3. He/she has to complete the steps and collect the data.
4. The data has to be analyzed and presented in a neat form (in a one/two page report). Any major deviations from theoretically predicted results to be explained by the student.
5. He/she has to appear for a viva to defend his/her results and close the experiment.

NOTE: No end semester lab reports will be entertained. Performance will be evaluated on weekly basis.

Chapter 1

Transmission Lines

1.1 To study the characteristics of a transmission line, to measure the VSWR for a waveguide section and to measure unknown load impedance

1.2 Theoretical background

A typical example of a transmission line can be the two wire parallel conductors. In any transverse plane the electric field lines pass from one to the other conductor while the magnetic field lines are perpendicular to the electric ones. The electric field lines define a voltage between the conductors while the magnetic field lines characterize the current flowing in the opposite directions in the two wires. The variation of the electric field induces a magnetic field and vice versa, resulting in a wave propagating along the line. In what follows we present a description for an idealized transmission line. Before that we list out the major issues to be discussed:

1. Energy propagation
2. Reflection at discontinuities
3. Standing wave vs. traveling wave and resonance properties of standing waves.
4. Phase and group velocities.
5. Effects of losses on wave propagation
6. Impedance matching and the Smith chart

1.2.1 Ideal transmission lines: spatio-temporal dependence of signals

Consider the transmission line shown in figure along with its distributed equivalent circuit. We ascribe an inductance and capacitance per unit length, denoted by L and C , respectively. Thus the length dz of the line will have an inductance Ldz and capacitance Cdz . The change in voltage across this elementary length can be written as

$$\frac{\partial V}{\partial z} dz = -(Ldz) \frac{\partial I}{\partial t}, \quad (1.1)$$

and for the current change we have

$$\frac{\partial I}{\partial z} dz = -(Cdz) \frac{\partial V}{\partial t}, \quad (1.2)$$

Canceling out the elementary length, one has

$$\frac{\partial V}{\partial z} = -L \frac{\partial I}{\partial t}, \quad (1.3)$$

$$\frac{\partial I}{\partial z} = -C \frac{\partial V}{\partial t}. \quad (1.4)$$

Eqns. (1.3) and (1.4) are the basic partial differential equations describing the evolution of voltage and current in the ideal (since there is no resistance Rdz) transmission line. These two equations can be combined to lead to wave equations for both current and voltage:

$$\frac{\partial^2 V}{\partial z^2} - \frac{1}{v^2} \frac{\partial^2 V}{\partial t^2} = 0, \quad (1.5)$$

$$\frac{\partial^2 I}{\partial z^2} - \frac{1}{v^2} \frac{\partial^2 I}{\partial t^2} = 0. \quad (1.6)$$

where $v^2 = 1/\sqrt{LC}$. The general solution of Eq.(1.5), for example, can be written as a superposition of forward and backward propagating waves with arbitrary profiles (check)

$$V(z, t) = F_1 \left(t - \frac{z}{v} \right) + F_2 \left(t + \frac{z}{v} \right) \quad (1.7)$$

and the corresponding solution for the current is given by

$$I(z, t) = \frac{1}{Lv} \left[F_1 \left(t - \frac{z}{v} \right) - F_2 \left(t + \frac{z}{v} \right) \right]. \quad (1.8)$$

We introduce a constant $Z_0 = Lv = \sqrt{L/C}$ as the characteristic impedance of the line. As is evident from Eq.(1.8) Z_0 has the dimensions of resistance.

Characteristic impedance and wave velocity for a coaxial line

Using the expressions of C and L for a coaxial segment the characteristic impedance can be written as

$$Z_0 = \frac{\ln b/a}{2\pi} \sqrt{\frac{\mu}{\varepsilon}}, \quad (1.9)$$

where a and b are the radii of the inner and outer conductors. For a commercial coaxial line, relative dielectric permittivity = 2.26, radii are $a = 0.406 \text{ mm}$, $b = 1.48 \text{ mm}$ and by setting $\mu = \mu_0$, one has $Z_0 = 51.6 \Omega$. The wave velocity is given by $v = 1/\sqrt{LC} = 1/\sqrt{\varepsilon\mu}$, which is the same as in the dielectric. It is usually $0.5 - 0.7 c$.

1.2.2 Reflection and transmission at a resistive discontinuity

One of the major problems in transmission lines involves junctions between a given line and another one of different characteristics. Due to the discontinuity part of the incident wave will always be reflected back. By Kirchhoff's law the total voltage and current must be continuous across the discontinuity. Thus the total voltage can be written as

$$V_+ + V_- = V_L \quad (1.10)$$

where V_+ (V_-) is the voltage corresponding to the forward (backward) traveling wave at the point of discontinuity. The sum of these two must be equal to the voltage V_L appearing across the junction. In an analogous fashion one has

$$I_+ + I_- = I_L \quad (1.11)$$

Consider now two cases. The first one corresponds to the simplest possible situation a load resistance R_L is connected at the point of discontinuity. The second corresponds to a ideal transmission line is connected to a second transmission line of infinite length and characteristic impedance Z_{0L} . For this case $R_L = Z_{0L}$ Many

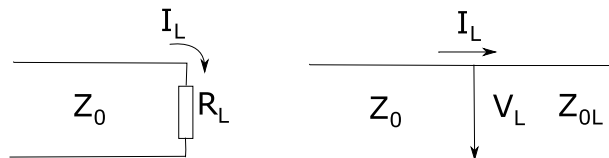


Figure 1.1: Resistive load and junction between two transmission lines.

other forms of load circuit can produce an effective resistance R_L at junction. In

all these cases

$$V_L = R_L I_L \quad (1.12)$$

Using the relation between the voltage and current Eq.(1.11) can be transformed into

$$\frac{V_+}{Z_0} - \frac{V_-}{Z_0} = \frac{V_L}{R_L} \quad (1.13)$$

Eqns. (1.10) and (1.13) can be used to calculate the reflection and the transmission coefficients as follows

$$\rho = \frac{V_-}{V_+} = \frac{R_L - Z_0}{R_L + Z_0} \quad (1.14)$$

$$\tau = \frac{V_L}{V_+} = \frac{2R_L}{R_L + Z_0} \quad (1.15)$$

It can be easily seen from Eq.(1.14) that for matched load, i.e., $R_L = Z_0$, there is no reflection. All energy of the incident wave is then transferred to the load and τ is then unity. The instantaneous incident power is given by

$$W_T^+ = I_+ V_+ = \frac{V_+^2}{Z_0} \quad (1.16)$$

and the fractional power reflected is given by

$$\frac{W_T^-}{W_T^+} = \rho^2. \quad (1.17)$$

The remaining power goes into the load resistance

$$\frac{W_{TL}}{W_T^+} = 1 - \rho^2. \quad (1.18)$$

1.2.3 Sinusoidal waves on ideal transmission lines

Let a sine voltage be applied at $z = 0$. Thus

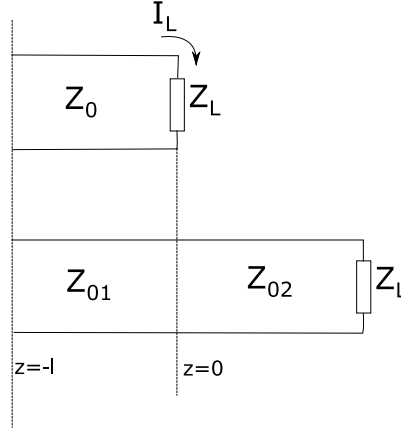
$$V(0, t) = V \cos \omega t \quad (1.19)$$

The corresponding wave traveling in the positive direction is

$$V_+(z, t) = |V_+| \cos \omega(t - z/v_p) \quad (1.20)$$

For the opposite direction we have

$$V_-(z, t) = |V_-| \cos \omega[(t + z/v_p) + \theta_p] \quad (1.21)$$

Figure 1.2: Typical situation with a discontinuity at $z = 0$.

The total voltage and current at any section z are then given by

$$V(z, t) = |V_+| \cos \omega(t - z/v_p) + |V_-| \cos \omega[t + z/v_p + \theta_p] \quad (1.22)$$

$$I(z, t) = \frac{|V_+|}{Z_0} \cos \omega(t - z/v_p) - \frac{|V_-|}{Z_0} \cos \omega[t + z/v_p + \theta_p] \quad (1.23)$$

For sinusoidal time variation write (1.22) and (1.23) in phasor form as

$$V(z, t) = V_+ e^{-j\beta z} + V_- e^{j\beta z}, \quad (1.24)$$

$$I(z, t) = \frac{1}{Z_0} (V_+ e^{-j\beta z} - V_- e^{j\beta z}), \quad (1.25)$$

where the phase constant $\beta = \omega/v = \omega\sqrt{LC}$. We can take V_+ to be real considering it to be real with zero phase. In general V_- will be complex given by

$$V_- = |V_-| e^{j\theta_p}. \quad (1.26)$$

βz measures the instantaneous phase at z with respect to $z = 0$. It is clear that both V and I are periodic in z with period $2\pi/\beta$ (called the wavelength λ).

Reflection and transmission coefficients for sinusoidal waves

Impedance for time-varying fields is defined as the ratio of total phasor voltage to the total phasor current at any point. We set this impedance at $z = 0$, the load impedance Z_L . We get from Eqs. (1.24) and (1.25) the expressions of the reflection and transmission coefficients

$$\rho = \frac{V_-}{V_+} = \frac{Z_L - Z_0}{Z_L + Z_0} \quad (1.27)$$

$$\tau = \frac{V_L}{V_+} = \frac{2Z_L}{Z_L + Z_0}, \quad (1.28)$$

The load voltage is the total voltage at $z = 0$. The expressions for power reflected and transmitted can be written as

$$\frac{W_T^-}{W_T^+} = |\rho|^2. \quad (1.29)$$

$$\frac{W_{TL}}{W_T^+} = 1 - |\rho|^2. \quad (1.30)$$

We can define input impedance and admittance at $z = -l$ by dividing (1.24) by (1.25).

$$Z_i = Z_0 \left[\frac{e^{j\beta l} + \rho e^{-j\beta l}}{e^{j\beta l} - \rho e^{-j\beta l}} \right] \quad (1.31)$$

$$= Z_0 \left[\frac{(Z_L + Z_0)e^{j\beta l} + (Z_L - Z_0)e^{-j\beta l}}{(Z_L + Z_0)e^{j\beta l} - (Z_L - Z_0)e^{-j\beta l}} \right] \quad (1.32)$$

$$= Z_0 \left[\frac{Z_L \cos \beta l + jZ_0 \sin \beta l}{Z_0 \cos \beta l + jZ_L \sin \beta l} \right]. \quad (1.33)$$

One can define admittance as the inverse of impedance as $Y_i = 1/Z_i$, $Y_0 = 1/Z_0$, and $Y_L = 1/Z_L$, so that

$$Y_i = Y_0 \left[\frac{Y_L \cos \beta l + jY_0 \sin \beta l}{Y_0 \cos \beta l + jY_L \sin \beta l} \right] \quad (1.34)$$

Standing wave ratio

As mentioned earlier, one constant in Eq.(1.24), eg., V_+ can be taken as real by choice of origin in time, so that the other becomes $V_- = V_+ |\rho| e^{j(\theta_p + \beta z)}$. Writing this as a real function at $z = -l$, we have

$$V(t, -l) = V_+ \cos(\omega t + \beta l) + V_+ |\rho| \cos(\omega t - \beta l + \theta_p) \quad (1.35)$$

It is clear that starting from $t = 0$, the phase of the first term (incident wave) increases with distance from $z = 0$, while that for the reflected wave decreases (see figure 1.3). Noting that $V_{max} = |V_+| + |V_-|$ and $V_{min} = |V_+| - |V_-|$, the standing wave ratio is defined as

$$S = \frac{V_{max}}{V_{min}} = \frac{|V_+| + |V_-|}{|V_+| - |V_-|} = \frac{1 + |\rho|}{1 - |\rho|} \quad (1.36)$$

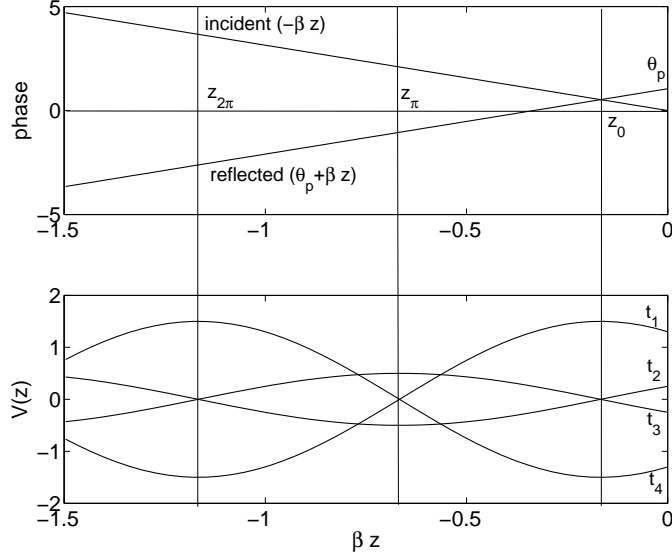


Figure 1.3: (a) Phase of the incident and reflected light at $t = 0$. (b) Total voltage $V(z)$ as function of βz (in units of π) at times $\omega t_1 = -\theta_p/2$, $\omega t_2 = -\theta_p/2 + \pi/2$, $\omega t_3 = -\theta_p/2 + \pi$ and $\omega t_4 = -\theta_p/2 + 3\pi/2$.

ρ can be expressed in terms of S as

$$|\rho| = \frac{S - 1}{S + 1}. \quad (1.37)$$

It is clear that maximum voltage corresponds to the minimum current

$$I_{min} = \frac{|V_+| - |V_-|}{Z_0} \quad (1.38)$$

At this point the impedance is resistive

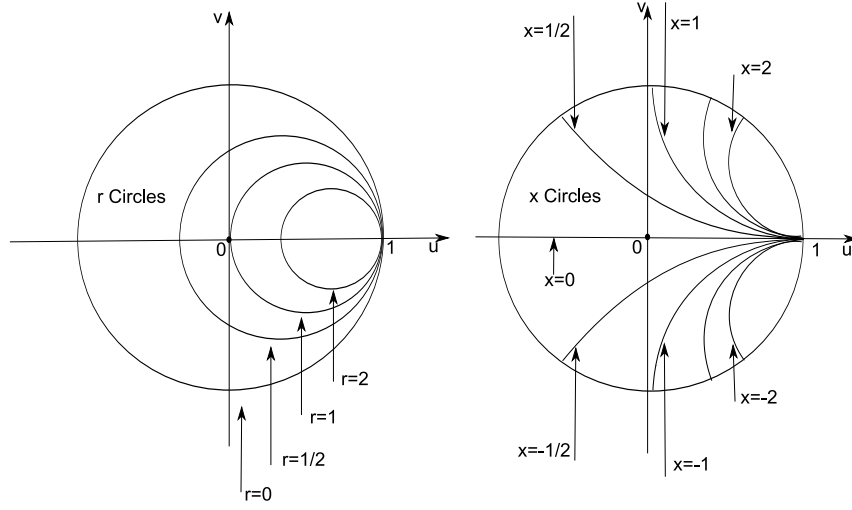
$$Z_{max} = Z_0 \frac{|V_+| + |V_-|}{|V_+| - |V_-|} = Z_0 S \quad (1.39)$$

At positions of voltage minimum current is maximum

$$I_{max} = \frac{|V_+| + |V_-|}{Z_0} \quad (1.40)$$

At this point the impedance is minimum and real

$$Z_{min} = Z_0 \frac{|V_+| - |V_-|}{|V_+| + |V_-|} = Z_0/S \quad (1.41)$$

Figure 1.4: r and x circles of a Smith chart.

1.2.4 The Smith chart for a transmission line

Definition and description

The Smith chart represents a family of curves which are the loci of constant resistance and reactance plotted on a polar diagram. In this diagram the radius corresponds to the magnitude of the reflection coefficient while the angle corresponds to the phase of the reflection coefficient. It is a beautiful example of the application of conformal mapping of the theory of complex variables (go back and check up what is conformal mapping). Some of the applications of the Smith chart, for example, is to find how impedances are transformed along the line or to relate the impedance to reflection coefficient or to standing wave ratio.

Define a normalized impedance

$$\zeta(l) = (r + jx) = \frac{Z_i}{Z_0} \quad (1.42)$$

We also define a complex variable w = reflection coefficient at the end of the line shifted in phase to correspond to the input position $-l$

$$w = u + jv = \rho e^{-2j\beta l} \quad (1.43)$$

$$Z_i = Z_0 \frac{e^{j\beta l} + \rho e^{-j\beta l}}{e^{j\beta l} - \rho e^{-j\beta l}} \Rightarrow \zeta(l) = \frac{1 + \rho e^{-2j\beta l}}{1 - \rho e^{-2j\beta l}} = \frac{1 + w}{1 - w} \quad (1.44)$$

$$= \frac{1 + (u + jv)}{1 - (u + jv)} \quad (1.45)$$

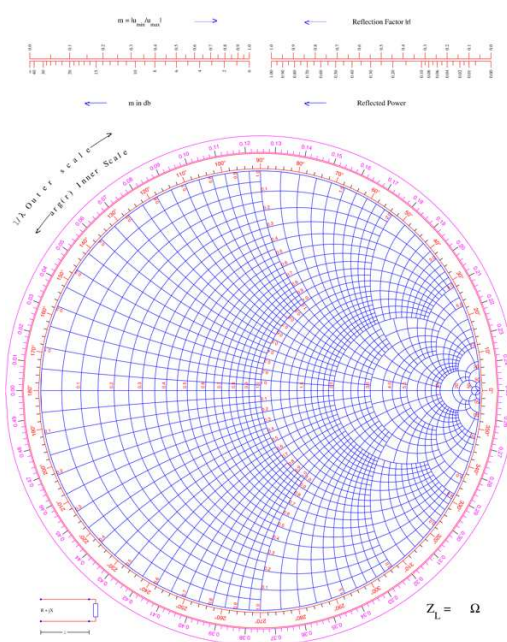


Figure 1.5: Smith Chart.

$$r + jx = \frac{1 + (u + jv)}{1 - (u + jv)}, \quad (1.46)$$

where resistance and reactance are given by

$$r = \frac{1 - (u^2 + v^2)}{(1 - u)^2 + v^2} \quad (1.47)$$

$$x = \frac{2v}{(1 - u)^2 + v^2}, \quad (1.48)$$

or

$$\left(u - \frac{r}{1+r}\right)^2 + v^2 = \frac{1}{(1+r)^2} \quad (1.49)$$

$$(u-1)^2 + \left(v - \frac{1}{x}\right)^2 = \frac{1}{x^2}. \quad (1.50)$$

Let us now plot the loci of constant resistance r on the w plane (u, v plane). These represent circles with centers at $[r/(1+r), 0]$ and with radius $1/(1+r)$.

$$\text{centre : } u_c = \frac{r}{1+r}, \quad v_c = 0 \quad (1.51)$$

$$\text{radius : } = \frac{1}{1+r} \quad (1.52)$$

r	0	$\frac{1}{2}$	1	2	∞
u_c	0	$\frac{1}{3}$	$\frac{1}{2}$	$\frac{2}{3}$	1
rad	1	$\frac{2}{3}$	$\frac{1}{2}$	$\frac{1}{3}$	0

For the loci of constant reactance x on the w plane, we have

$$centre : \quad u_c = 1, \quad v_c = \frac{1}{x} \quad (1.53)$$

$$radius : \quad = \frac{1}{|x|} \quad (1.54)$$

x	0	$\pm\frac{1}{2}$	± 1	± 2	∞
v_c	∞	± 2	± 1	$\pm\frac{1}{2}$	0
rad	∞	± 2	± 1	$\pm\frac{1}{2}$	0

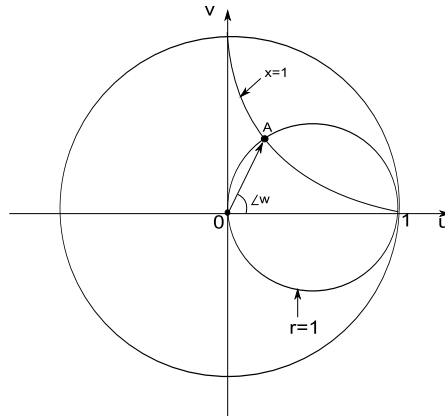


Figure 1.6: block diagram.

1.2.5 Uses of Smith Chart

To find reflection coefficient for given load impedance or vice versa

Point A in Fig.1.6. is the intersection of circles $x = 1$ and $r = 1$ implying a normalized impedance of $1 + 1j$. By definition we have

$$\begin{aligned} w &= \rho e^{-2j\beta l} \\ |w| &= |\rho| \\ |w| &= (u^2 + v^2)^{\frac{1}{2}}. \end{aligned}$$

Note that

$$|w| = (u^2 + v^2)^{\frac{1}{2}} = 1 \quad (1.55)$$

on the $r = 0$ circle. Thus a measure of the radius to some point on the graph as a fraction of radius to $r = 0$ circle yields $|\rho|$ directly. If the point on the Smith chart represents the normalized load impedance, i.e., $l = 0$, $\angle w = \angle \rho$, the phase angle of the reflection coefficient can be read directly from the chart. The angle may be determined by reading the outside wavelength markings appreciating that a quarter wave corresponds to π radians.

Example:

Suppose a transmission line of characteristic impedance $z_0 = 70 \Omega$ is terminated with a load $z_L = 70 + 70j \Omega$, so that the normalized load impedance $\zeta(0) = 1 + 1j$ (same point A) with $|\rho| = 0.45$ and $\angle \rho = \angle w = 1.11 \text{ rad}$. It is understood that the reverse calculation of the load impedance for a given complex reflection coefficient can also be carried out.

Transformation of impedance along a line

Let l be the position along the line measured w.r.t. load. A change in l corresponds to a change in the phase angle of w ($-2\beta l$). Regarding the direction we will follow the following convention. Moving toward the generator (increasing l) will correspond to an increase in the phase of w in the negative direction. This will correspond to clockwise movement. On the contrary, moving towards the load will correspond to anti clockwise rotation.

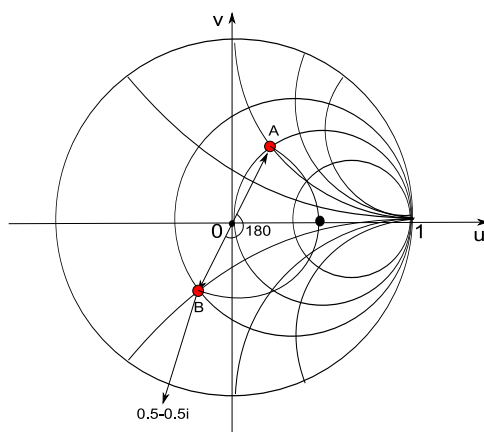


Figure 1.7: Change of impedance along a line.

Example:

Let the normalized load impedance be $1 + 1j$ (point A in Fig.1.7). If the line is a quarter wave long, then we move towards the generator by π at constant radius, i.e., $\beta l = 90^\circ$ and $2\beta l = 180^\circ$. Thus the reading from chart for input impedance is $\zeta(l) = 0.5 - 0.5j$. If input impedance is given and load impedance is required to be found out, the reverse procedure can be used.

Standing wave ratio and position of voltage maximum

Let a transmission line with a known load impedance is given (say, point A in Fig.1.8) and we have to find out the standing wave ratio. Noting that the location of maximum impedance is also the voltage maximum (and current minimum) with both real, it can be easily deduced that the maximum impedance for an ideal transmission line is real, i.e., it is a pure resistance point (lies on u -axis of the w -plane). Thus the standing wave ratio S

$$S = \frac{V_{max}}{V_{min}} = \frac{V_{max}}{Z_0 I_{min}} = \frac{Z_{max}}{Z_0} \quad (1.56)$$

is given by point C ($x = 0, r = Z_{max}$) on u -axis. The value of the normalized resistance at C gives the standing wave ratio. For example, for a load impedance $1 + 1j$ one has to move clockwise to the generator by 0.088λ to reach point C, where the normalized resistance is 2.6 which is the same as the SWR.

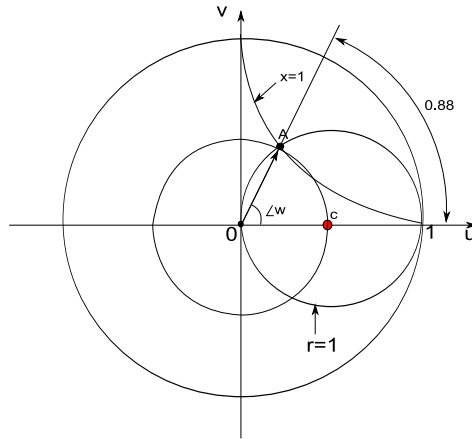


Figure 1.8: Standing wave ratio from known load resistance.

Example: Impedance transformation along cascaded lines

Work out the Example 5.10e of [2].

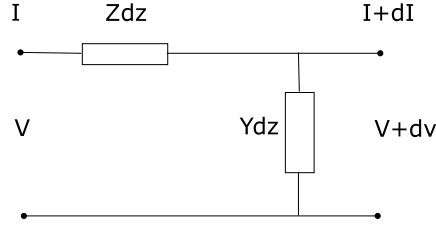


Figure 1.9: Schematics of a lossy/general transmission line.

1.2.6 Transmission lines with general forms of distributed impedance (Lossy lines)

Very often the transmission lines are lossy and their equivalent circuitry can be complex. For lossy lines or for filter type lines, the series element can be represented by a generalized distributed impedance Z per unit length, while the distributed shunt element by an admittance Y per unit length. The corresponding equations can be written as

$$\frac{dV}{dz} = -ZI \quad (1.57)$$

$$\frac{dI}{dz} = -YV \quad (1.58)$$

and they can be reduced to second order ODE's as

$$\frac{d^2V}{dz^2} = \gamma^2 V, \quad (1.59)$$

$$\frac{d^2I}{dz^2} = \gamma^2 I. \quad (1.60)$$

Here $\gamma = \sqrt{ZY}$. The solution for V and I can be written as

$$V = V_+ e^{-\gamma z} + V_- e^{\gamma z}, \quad (1.61)$$

$$I = \frac{1}{Z_0} (V_+ e^{-\gamma z} - V_- e^{\gamma z}). \quad (1.62)$$

where Z_0 is given by

$$Z_0 = \frac{Z}{\gamma} = \sqrt{\frac{Z}{Y}}. \quad (1.63)$$

Note that in general the characteristic impedance Z_0 is complex, implying that the voltage and current are not in phase. The propagation constant γ is also complex (in general), leading to a damping of the waves as they propagate. One has to

exercise caution in using the proper sign for the propagation constant for forward and backward waves. Separating the real and imaginary parts of the propagation constant, i.e., by writing $\gamma = \alpha + j\beta = \sqrt{ZY}$, one can easily see the damped propagation of the waves

$$V = V_+ e^{-\alpha z} e^{-j\beta z} + V_- e^{\alpha z} e^{j\beta z} \quad (1.64)$$

It is clearly seen that α gives the rate of exponential decay or the attenuation constant, while β characterizes the phase shift gives the phase constant. As before the reflection coefficient is defined and calculated as

$$\rho = \frac{V_-}{V_+} \quad (1.65)$$

$$= \frac{Z_L - Z_0}{Z_l - Z_0} \quad (1.66)$$

One can also find the input impedance at $Z = -l$ in terms of reflection coefficient ρ at $Z = 0$ as

$$Z_i = \frac{V}{I} = Z_0 \left(\frac{V_+ e^{\gamma l} + V_- e^{-\gamma l}}{V_+ e^{\gamma l} - V_- e^{-\gamma l}} \right) \quad (1.67)$$

$$= Z_0 \left[\frac{1 + \rho e^{-2\gamma l}}{1 - \rho e^{-2\gamma l}} \right] \quad (1.68)$$

$$= Z_0 \left[\frac{Z_L \cosh \gamma l + Z_0 \sinh \gamma l}{Z_0 \cosh \gamma l + Z_L \sinh \gamma l} \right] \quad (1.69)$$

1.2.7 Transmission line with series and shunt losses

Let the impedance and admittance be given by

$$Z = R + j\omega L \quad (1.70)$$

$$Y = G + j\omega C \quad (1.71)$$

One can use these equations to determine the propagation constants and the characteristic impedance. For many problems the following inequalities hold

$$\frac{R}{\omega L} \ll 1, \quad \frac{G}{\omega C} \ll 1. \quad (1.72)$$

Retaining up to the second-order terms in these small parameters, one can have the expressions for all the relevant quantities α , β and Z_0 as

$$\alpha \approx \frac{R}{2\sqrt{\frac{L}{C}}} + \frac{G_0\sqrt{\frac{L}{C}}}{2} \quad (1.73)$$

$$\beta \approx \omega\sqrt{LC} \left[1 - \frac{RG}{4\omega^2 LC} + \frac{G^2}{8\omega^2 C^2} + \frac{R^2}{8\omega^2 L^2} \right] \quad (1.74)$$

$$Z_0 \approx \frac{L}{C} \left[\left(1 + \frac{R^2}{8\omega^2 L^2} - \frac{3G^2}{8\omega^2 C^2} + \frac{RG}{4\omega^2 LC} \right) + j \left(\frac{G}{2\omega C} - \frac{R}{2\omega L} \right) \right]. \quad (1.75)$$

Derivation of α from physical principles for low loss lines

The approximate result given by (1.73) can be obtained from simple physical arguments. Consider only the positive propagating wave

$$V = V_+ e^{-\alpha z} e^{-j\beta z} \quad (1.76)$$

$$I = I_+ e^{-\alpha z} e^{-j\beta z} \quad (1.77)$$

with average power transfer at any point given by

$$W_T = \frac{1}{2} V_+ I_+ e^{-2\alpha z} = \frac{1}{2} \text{Re}(VI^*) \quad (1.78)$$

Let the imaginary part of Z_0 be negligible, leading to V_+ in phase with I_+ . The rate of decrease of average power with distance must be equal to the average power loss W_L in the line per unit length.

$$\frac{\partial W_T}{\partial z} = -W_L = -2\alpha \left(\frac{1}{2} V_+ I_+ e^{-2\alpha z} \right) = -2\alpha W_T \quad (1.79)$$

$$\alpha = \frac{W_L}{2W_T} \quad (1.80)$$

Given the resistance R and the shunt conductance G , the average power loss per unit length W_L and W_T at $z = 0$ are given by

$$W_L = \frac{I_+^2 R}{2} + \frac{V_+^2 G}{2} = \frac{V_+^2}{2} \left(G + \frac{R}{Z_0^2} \right) \quad (1.81)$$

$$W_T = \frac{1}{2} V_+ I_+ = \frac{1}{2} \frac{V_+^2}{Z_0}, \quad (1.82)$$

leading to the expression of α

$$\alpha = \frac{1}{2} \left(G Z_0 + \frac{R}{Z_0} \right) \text{ Np/m}. \quad (1.83)$$

One neper (Np) per meter indicates that the amplitude has decayed to $1/e$ of its incoming value in 1 m.

1.2.8 Resonant transmission lines

Pure standing waves on a transmission line

Let an ideal transmission line be shorted at one end $z = 0$. For such a line $S = \infty$, $|\rho| = 1$, $|V_-| = |V_+|$ and the following relations hold

$$V(0) = V_+ + V_- = 0, \quad V_+ = -V_- \quad (1.84)$$

$$V(z) = V_+ (e^{-j\beta z} - e^{j\beta z}) = -2jV_+ \sin \beta z \quad (1.85)$$

$$I = \frac{V_+}{Z_0} (e^{-j\beta z} + e^{j\beta z}) = 2\frac{V_+}{Z_0} \cos \beta z \quad (1.86)$$

Thus one can make the following observations:

1. Voltage is zero not only at $z = 0$ but also at all points where βz is a multiple of π .
2. Voltage is maximum at odd multiples of $\pi/2$.
3. Current is maximum at short circuit and at all points where voltage is zero.
4. Ratio between maximum current and the maximum voltage is Z_0

1.3 Experiment for VSWR measurement

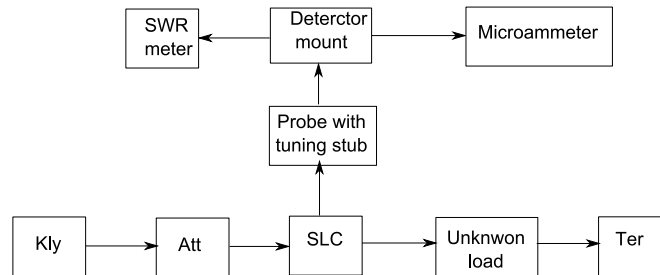


Figure 1.10: VSWR measurement.

1.3.1 Experimental procedure:

One distinguishes between two cases, namely, the regime of low (< 10) and high (> 10) VSWR. We discuss them separately.

Small VSWR (< 10)

1. Arrange the equipment as shown in Fig1.10. with a load terminated at its end.
2. Tune the detector by adjusting its length inside the waveguide for maximum meter deflection.
3. Insert the element under test and measure the distance between two adjacent minima to calculate λ and the frequency (distance between adjacent minima is $\lambda_g/2$).
4. Move the probe along the slotted line to obtain maximum and minimum current readings on the microammeter.
5. Calculate *VSWR* as

$$VSWR = \frac{I_{max}}{I_{min}} \quad (1.87)$$

6. If SWR meter is used, adjust its gain to give full scale deflection to read 1.00 when the detector is at voltage maximum. Move the probe along the slotted line and when the detector is at voltage minimum, SWR meter gives directly the *VSWR*.

Large VSWR (> 10)

1. Move the probe to get the minimum current and record it.
2. Move the probe on both sides of this minimum to find the positions x_1 (towards generator) and x_2 (towards load) where the meter readings are double of the minimum reading.
3. Measure the *VSWR* in this case as

$$VSWR = \frac{\lambda}{\pi(x_2 - x_1)} \quad (1.88)$$

4. If SWR meter is used, adjust its gain to give $3dB$ deflection when the detector is at voltage minimum. Find the positions of x_1 and x_2 where the SWR meter shows $0.00dB$. Now use the above formula to find *VSWR*

1.3.2 Measuring the unknown load impedance:

As discussed in chapter1, the waves incident on the load from the generator is reflected. So the phase and the position of the minima are the characteristic properties of the load. See Eq.(1.33)for the input impedance

$$Z_i = Z_0 \left[\frac{Z_L \cos \beta l + j Z_0 \sin \beta l}{Z_0 \cos \beta l + j Z_L \sin \beta l} \right]. \quad (1.89)$$

Where Z_L is the impedance at the receiving end. Z_i is the characteristic impedance and βl is the electrical distance is measured in wavelengths between position of termination and standing wave minimum. Here

$$\beta l = \frac{2\pi}{\lambda}(x_2 - x_1) \quad (1.90)$$

and Z_i corresponding to Z_{min} hence from Eq.1.39,

$$S = \frac{Z_0}{Z_i} \quad (1.91)$$

Re arranging Eq.1.89,we get

$$\begin{aligned} Z_L(Z_0 \cos \beta l - j Z_i \sin \beta l) &= Z_0(Z_i \cos \beta l - j Z_0 \sin \beta l) \\ \frac{Z_L}{Z_0} &= \frac{Z_i \cos \beta l - j Z_0 \sin \beta l}{Z_0 \cos \beta l - j Z_i \sin \beta l} \\ &= \frac{\cos \beta l - j S \sin \beta l}{S \cos \beta l - j \sin \beta l} \end{aligned} \quad (1.92)$$

where S is VSWR reading

1.3.3 Procedure

1. Arrange the equipment and insert the unknown load. Repeat the above steps to find $VSWR$.
2. Find the position of any standing wave minimum and record it as x_1 . (This is the position of the reference minimum.
3. Replace the load by short-circuit termination and move the probe carriage to new standing wave minimum x_2 .
4. Find the shift in the minimum $l = (x_2 - x_1)$. Hence calculate $\beta l = \frac{2\pi}{\lambda}(x_2 - x_1)$
5. Use Eq.1.92 to estimate the impedance of the load.

1.3.4 Estimation of normalized load using Smith chart

1. Obtain the $VSWR$ and the shift in the minima ($x_2 - x_1$) for the unknown load as explained in the above section.
2. Since $VSWR = Z_{max}/Z'_0$, where Z'_0 is the characteristic impedance of the waveguide, find the circle $r=VSWR$ (where r is the real part of $\zeta = r + jx$) on the normalized Smith chart. And find the point of intersection with $u - axis$.
3. Draw a circle with origin ($u = 0, v = 0$) as its center and passing through this point.
4. Locate a point on the perimeter of the Smith chart at a distance equal to βl (see Eq.1.90) from the point 0.00 moving in anti-clockwise direction (towards load) if the shift is positive. Draw a line connecting this point and the origin ($u=0, v=0$).
5. Note the point of intersection of this circle and this line. Obtain reactive and resistive components of the load from the reactive and real circles, respectively for this this point. That gives the normalized load impedance. The actual load impedance is given by

$$Z_L = Z'_0(r + jx) \quad (1.93)$$

Z'_0 , the characteristic impedance of the wave guide, is given by

$$Z'_0 = Z_0 \frac{\lambda_g}{\lambda_0} \cdot \frac{b}{a} \quad (1.94)$$

here Z_0 is the impedance of the free space $=\sqrt{\mu_0/\epsilon_0} = 377 \Omega$

6. Calculate using measured Z_L from Eq.1.93, the reflection coefficient

$$|\rho| = \left| \frac{Z_L - Z'_0}{Z_L + Z'_0} \right| \quad (1.95)$$

and hence VSWR. Compare this VSWR with the measured value

Chapter 2

Wave guides

2.1 General formulation for guided waves

Consider a cylindrical system with axis along z (see figure) characterized by a propagation factor $e^{j\omega t - \gamma z}$. Assume no net charge or current density inside the cylindrical tube, i.e., $\rho = 0$, $\vec{J} = 0$. Propagation constant γ determines the properties of the waves. The phasor wave equations can be written as

$$\nabla^2 \vec{E} = -k^2 \vec{E} \quad (2.1)$$

$$\nabla^2 \vec{H} = -k^2 \vec{H} \quad (2.2)$$

$$\nabla^2 \vec{E} = \nabla_t^2 \vec{E} + \frac{\partial^2 \vec{E}}{\partial z^2} \quad (2.3)$$

The first term in the right hand side of Eq.(2.3) gives the transverse variation, while the second term corresponds to the axial variation.

$$\frac{\partial^2 \vec{E}}{\partial z^2} = \gamma^2 \vec{E} \quad (2.4)$$

$$\nabla^2 \vec{E} = -k^2 \vec{E} \quad (2.5)$$

$$\nabla_t^2 \vec{E} + \gamma^2 \vec{E} = -k^2 \vec{E} \quad (2.6)$$

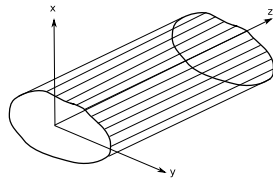


Figure 2.1: Schematics of a cylindrical wave guide.

Transverse variation must satisfy these two equations.

$$\nabla_t^2 \vec{E} = -(k^2 + \gamma^2) \vec{E} \quad (2.7)$$

$$\nabla_t^2 \vec{H} = -(k^2 + \gamma^2) \vec{H} \quad (2.8)$$

Assuming the phase factor to be $e^{j\omega t - \gamma z}$ the curl equation $\nabla \times \vec{E} = -j\omega\mu\vec{H}$ can be written in the component form as

$$\frac{\partial E_z}{\partial y} + \gamma E_y = -j\omega\mu H_x \quad (2.9)$$

$$-\gamma E_x - \frac{\partial E_z}{\partial x} = -j\omega\mu H_y \quad (2.10)$$

$$\frac{\partial E_y}{\partial x} + \gamma E_x = -j\omega\mu H_z \quad (2.11)$$

Similarly the other curl equation $\nabla \times \vec{H} = j\omega\epsilon\vec{E}$ can be decomposed into the components as

$$\frac{\partial H_z}{\partial y} + \gamma H_y = j\omega\epsilon E_x \quad (2.12)$$

$$-\gamma H_x - \frac{\partial H_z}{\partial x} = j\omega\epsilon E_y \quad (2.13)$$

$$\frac{\partial H_y}{\partial x} + \gamma H_x = -j\omega\epsilon E_z \quad (2.14)$$

Eqs. (2.9)-(2.14) can be solved for E_x , E_y , H_x , H_y in terms of E_z and H_z . (Example: H_x is found from (2.9) and (2.13).

$$E_x = -\frac{1}{k^2 + \gamma^2} \left(\gamma \frac{\partial E_z}{\partial x} + j\omega\mu \frac{\partial H_z}{\partial y} \right) \quad (2.15)$$

$$E_y = \frac{1}{k^2 + \gamma^2} \left(-\gamma \frac{\partial E_z}{\partial y} + j\omega\mu \frac{\partial H_z}{\partial x} \right) \quad (2.16)$$

$$H_x = \frac{1}{k^2 + \gamma^2} \left(j\omega\epsilon \frac{\partial E_z}{\partial y} - \gamma \frac{\partial H_z}{\partial x} \right) \quad (2.17)$$

$$H_y = -\frac{1}{k^2 + \gamma^2} \left(j\omega\epsilon \frac{\partial E_z}{\partial x} + \gamma \frac{\partial H_z}{\partial y} \right) \quad (2.18)$$

For propagating waves it is useful to use $\gamma = j\beta$ with β real in absence of attenuation and (2.15)-(2.18) reduce to

$$E_x = -\frac{j}{k_c^2} \left(\beta \frac{\partial E_z}{\partial x} + \omega\mu \frac{\partial H_z}{\partial y} \right), \quad (2.19)$$

$$E_y = \frac{j}{k_c^2} \left(-\beta \frac{\partial E_z}{\partial y} + \omega \mu \frac{\partial H_z}{\partial x} \right), \quad (2.20)$$

$$H_x = \frac{j}{k_c^2} \left(\omega \epsilon \frac{\partial E_z}{\partial y} - \beta \frac{\partial H_z}{\partial x} \right), \quad (2.21)$$

$$H_y = -\frac{j}{k_c^2} \left(\omega \epsilon \frac{\partial E_z}{\partial x} + \beta \frac{\partial H_z}{\partial y} \right), \quad (2.22)$$

where $k_c^2 = k^2 + \gamma^2 = k^2 - \beta^2$.

2.1.1 Classification of the waves

We can now classify the waves as

1. TEM waves: with $E_z = 0, H_z = 0$. Usually they exist in multi conductor guides.
2. TM waves: $E_z \neq 0, H_z = 0$.
3. TE waves: $E_z = 0, H_z \neq 0$.
4. Hybrid waves: here the boundary conditions require all field components.

2.2 Cylindrical waveguiding with various cross sections

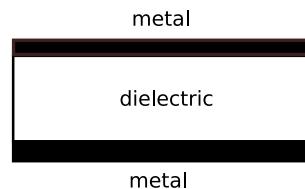


Figure 2.2: Cross-section of a metal strip waveguide.

2.2.1 Metal parallel plate guide

TEM waves

Metal strip guides (see Fig.2.2) can be considered as the simplest example of a guide supporting TEM waves. Usually they represent two-conductor transmission

lines. Non-zero fields are possible only if $\gamma^2 + k^2 = 0$ implying $\gamma_{TEM} = \pm jk$. Both electric and magnetic fields satisfy Laplace's equation (as in electrostatics) with fields propagating at the speed of light.

$$\nabla_t^2 \vec{E} = 0 \quad (2.23)$$

$$\nabla_t^2 \vec{H} = 0 \quad (2.24)$$

These equations yield uniform electric field between two parallel plate conductors with

$$E_x = E_0. \quad (2.25)$$

The corresponding magnetic field is given by

$$H_y = \frac{\gamma}{j\omega\mu} E_x = \pm \frac{j\omega\sqrt{\mu\epsilon}}{j\omega\mu} E_x = \pm \sqrt{\frac{\epsilon}{\mu}} E_x. \quad (2.26)$$

where the \pm corresponds to forward and backward propagating waves, respectively.

TM Waves

For transverse magnetic modes, $E_z \neq 0$, $H_z = 0$ and they can be supported in the parallel plate conducting guide. Assuming the system to be infinite in the y direction ($\frac{\partial}{\partial y} = 0$), we have

$$\nabla_t^2 E_z = -k_c^2 E_z = (k^2 + \gamma^2) E_z \quad (2.27)$$

$$\frac{\partial^2 E_z}{\partial x^2} = -k_c^2 E_z, \quad (2.28)$$

where $k_c^2 = k^2 + \gamma^2 = k^2 - \beta^2$. For the solution we have

$$E_z(z) = A \sin k_c x + B \cos k_c x. \quad (2.29)$$

For perfect conductors the tangential component of E , i.e., E_z must be equal to zero at the metal surface. Applying the boundary conditions at faces at $x = 0$, $x = a$, we obtain $B = 0$, $k_c a = m\pi$, $m = 1, 2, 3$ leading to

$$E_z = A \sin \frac{m\pi x}{a} \quad (2.30)$$

Other components are found to be

$$E_x = -\frac{1}{k^2 + \gamma^2} \left(\gamma \frac{\partial E_z}{\partial x} \right) \quad (2.31)$$

$$= -\frac{\gamma}{k_c^2} \frac{m\pi}{a} A \cos \frac{m\pi x}{a} \quad (2.32)$$

$$= -\frac{\gamma a}{m\pi} A \cos \frac{m\pi x}{a} \quad (2.33)$$

2.2. CYLINDRICAL WAVEGUIDING WITH VARIOUS CROSS SECTIONS 33

For the magnetic field components we have $H_z = 0$, $H_x = 0$ and H_y can easily be calculated.

It is clear that there is an infinite number of solutions for various values of m , each with a different field distributions. These are referred to as the *modes* (in this case TM modes) of the structure. The propagation constant of a given mode is given by

$$\gamma = \sqrt{k_c^2 - k^2} = \sqrt{\left(\frac{m\pi}{a}\right)^2 - \omega^2\mu\epsilon} \quad (2.34)$$

At sufficiently high frequencies

$$\gamma = j\beta = j\omega\sqrt{\mu\epsilon}\sqrt{1 - \left(\frac{\left(\frac{m\pi}{a}\right)^2}{\omega^2\mu\epsilon}\right)} \quad (2.35)$$

and the phase constant approaches that of a plane wave as $\omega \rightarrow \infty$. Lowering the frequency one can achieve $\gamma = 0$ at ω_c , which is given by the expression

$$\omega_c = \frac{m\pi}{a} \frac{1}{\sqrt{\mu\epsilon}} = \frac{m\pi v}{a} \quad (2.36)$$

ω_c is the cut-off frequency, v is the velocity of light ($= 1/\sqrt{\mu\epsilon}$). Propagation takes place only when β is real requiring $\omega > \omega_c$

$$\gamma = j\beta = j\omega\sqrt{\mu\epsilon}\sqrt{1 - \left(\frac{\omega_c}{\omega}\right)^2} \quad (2.37)$$

$$\beta = k\sqrt{1 - \left(\frac{\omega_c}{\omega}\right)^2} \quad (2.38)$$

For $\omega < \omega_c$, one can define the attenuation constant α as

$$\alpha = \gamma = \frac{m\pi}{a}\sqrt{1 - \left(\frac{\omega}{\omega_c}\right)^2} \quad (2.39)$$

$$\left(\frac{\alpha}{\omega_c\sqrt{\epsilon\mu}}\right)^2 = \frac{\omega_c^2 - \omega^2}{\omega^2} \quad (2.40)$$

Corresponding to the cut-off frequency, one can define a cut-off wave length as

$$\lambda_c = \frac{2\pi v}{\omega_c} = \frac{2a}{m} \quad (2.41)$$

Thus cut-off for the m -th mode occurs when the spacing between the plates is m times half wavelength. TM waves can propagate above a cut off frequency, equivalently, at wavelengths shorter than the cut-off wave length.

At lower frequencies $\omega < \omega_c$, γ is real and there is attenuation without any phase shift. At frequencies above the cut-off (i.e., for propagating modes) one can define the phase and group velocities of the modes:

Phase velocity

$$v_p = \frac{\omega}{\beta} = \frac{v}{\sqrt{1 - \left(\frac{\omega_c}{\omega}\right)^2}} > v \quad (2.42)$$

Group velocity

$$v_g = \frac{\partial\omega}{\partial\beta} = v\sqrt{1 - \left(\frac{\omega_c}{\omega}\right)^2} < v \quad (2.43)$$

Thus, the phase velocity is always greater than velocity of light in the medium, while the group velocity is always less. At $\omega = \omega_c$ there is no group propagation. Both the velocities approach the same value when $\omega \gg \omega_c$.

2.2.2 TM waves in a rectangular guide

The most often used guide in the microwave domain is the rectangular guide in the form of a hollow pipe. There can be no TEM wave in a hollow pipe bounded by a single conductor (why?). The solution for E_z for this case can be written as

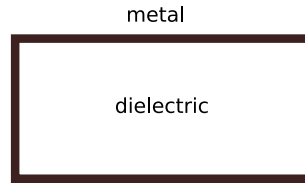


Figure 2.3: Cross-section of a rectangular waveguide.

$$E_z = A \sin k_x x \sin k_y y, \quad (2.44)$$

where due to boundary conditions, k_x and k_y must satisfy

$$k_x a = m\pi, \quad k_y b = n\pi, \quad m, n = 1, 2, 3 \dots \quad (2.45)$$

Thus the cut-off frequency for the TM_{mn} mode becomes

$$\omega_{c\ mn} = \frac{k_{c\ mn}}{\sqrt{\varepsilon\mu}} = \frac{1}{\sqrt{\varepsilon\mu}} \left[\left(\frac{m\pi}{a}\right)^2 + \left(\frac{n\pi}{b}\right)^2 \right]^{1/2}, \quad (2.46)$$

2.2. CYLINDRICAL WAVEGUIDING WITH VARIOUS CROSS SECTIONS 35

where $k_c^2 = k_x^2 + k_y^2 = k^2 - \beta^2$. The attenuation and the propagation constants are given by

$$\alpha = k_{c\ mn} \sqrt{1 - \left(\frac{\omega}{\omega_{c\ mn}}\right)^2}, \quad \omega < \omega_{c\ mn} \quad (2.47)$$

$$\beta = k \sqrt{1 - \left(\frac{\omega_{c\ mn}}{\omega}\right)^2}, \quad \omega > \omega_{c\ mn} \quad (2.48)$$

The expressions for the phase and group velocities remain the same as in the previous case.

Chapter 3

Directional Coupler

3.1 Objectives

To measure the characteristics of the directional coupler such as coupling(C), directivity(D) and isolation(I).

3.2 Theoretical background

We first consider the general theory of the N-port waveguide junctions and develop the expression for the scattering matrix S . We then apply the theory to directional couplers and to E - plane, H - plane and magic tees in the next chapter.

3.2.1 N-port waveguide junctions

A typical N -port junction has N inputs $\{a_i, i = 1 : N\}$, and N outputs $\{b_i, i = 1 : N\}$. An example of a four port junction is shown in Fig.3.1. The output values can be linked to the inputs through the $N \times N$ scattering matrix $[S]$ as follows

$$[b] = [S][a], \quad (3.1)$$

so that the transfer from one port to the other can easily be judged by the elements of $[S]$. In the above equation $[a]$ and $[b]$ represent column vectors. For the network to be reciprocal, one has to demand that the matrix $[S]$ must be symmetric, i.e., $S_{ij} = S_{ji}$. For a loss free network the following conservation relation must hold

$$\sum_{m=1}^N b_m b_m^* = \sum_{m=1}^N a_m a_m^* \quad (3.2)$$

In matrix form we have

$$[b]_t [b^*] = [a]_t [a^*] \quad (3.3)$$

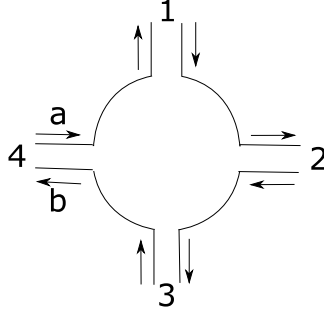


Figure 3.1: Block diagram of a directional coupler

Using Eq.(3.1), this can be written as

$$([S][a])_t[S^*][a^*] = [a]_t[a^*] \quad (3.4)$$

Since the transpose of a product is the product of the transposed, we have

$$[a_t][S_t][S^*][a^*] = [a]_t[U][a^*]. \quad (3.5)$$

where $[U]$ is the unit matrix. Finally we arrive at the unitarity property of $[S]$

$$[S_t][S^*] = [S^*][S_t] = [U]. \quad (3.6)$$

In terms of the elements the unitarity implies

$$\sum_{n=1}^N S_{in}S_{in}^* = 1, \quad (3.7)$$

$$\sum_{n=1}^N S_{in}S_{jn}^* = 0, \quad \text{for } i \neq j \quad (3.8)$$

3.2.2 Directional coupler as an example of a four-port junction

A directional coupler is a four-port component (see Fig(3.2)) in which two transmission lines are coupled in such a way that the output at a port of one transmission line depends on the direction of propagation in the other. Fig(3.3) illustrates two transmission lines coupled in the junction. As shown in the Fig(3.3) the waves crossing the center layer and entering into port-3 are in phase. On the other hand the waves towards port-4 are π out of phase as the distance between the successive holes is $\frac{\lambda}{4}$ and the path difference is two times $\frac{\lambda}{4}$. The line from port-1 to port-2 is

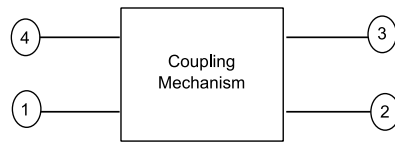


Figure 3.2: Block diagram of a directional coupler

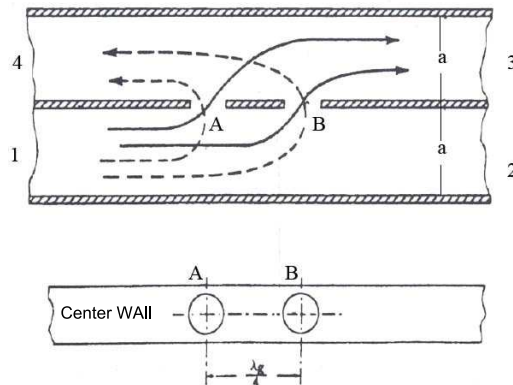


Figure 3.3: Coupling through the center wall of the guides.

coupled to the line from port-3 to port-4. In an ideal coupler, a signal entering port one will travel to port-2, and a predetermined portion of this signal will appear at one of the other two ports. There will be zero output at the fourth port. If the main signal travels in the reverse direction, from port-2 to port-1, a small coupled signal will appear at the port which was isolated in the first case. Frequently only three of the four ports are used in a microwave circuit. In this case the unwanted port is usually terminated by a matched load built into it. The component then looks like a three-port network but it is still a four-port network even though the fourth port is concealed.

The scattering matrix for the coupler can be written as

$$[S] = \begin{pmatrix} 0 & S_{12} & S_{13} & 0 \\ S_{12} & 0 & 0 & S_{24} \\ S_{13} & 0 & 0 & S_{34} \\ 0 & S_{24} & S_{34} & 0 \end{pmatrix} \quad (3.9)$$

Eq.(3.7) reduces to

$$i = 1, \quad |S_{12}|^2 + |S_{13}|^2 = 1 \quad (3.10)$$

$$i = 2, \quad |S_{12}|^2 + |S_{24}|^2 = 1 \quad (3.11)$$

$$i = 3, \quad |S_{13}|^2 + |S_{34}|^2 = 1 \quad (3.12)$$

$$i = 4, \quad |S_{24}|^2 + |S_{34}|^2 = 1 \quad (3.13)$$

Using Eq.(3.8) we have

$$i = 1, j = 4 \quad S_{12}S_{24}^* + S_{13}S_{34}^* = 0 \quad (3.14)$$

$$i = 2, j = 3 \quad S_{12}S_{13}^* + S_{24}S_{34}^* = 0. \quad (3.15)$$

Note that by virtue of reciprocity ($S_{ij} = S_{ji}$) and unitarity ($S_{ij}^* = S_{ji}$) all the elements of $[S]$ are real and using Eqs.(3.10)-(3.15) one can easily show that

$$S_{12} = S_{34} = \tilde{a} \quad (3.16)$$

$$S_{24} = -S_{13} = \tilde{b} \quad (3.17)$$

Here \tilde{a} and \tilde{b} carry the physical information about the transmission and the coupling, respectively. One can also show that $(\tilde{a})^2 + (\tilde{b})^2 = 1$ in absence of losses. The scattering matrix now looks as

$$[S] = \begin{pmatrix} 0 & \tilde{a} & -\tilde{b} & 0 \\ \tilde{a} & 0 & 0 & \tilde{b} \\ -\tilde{b} & 0 & 0 & \tilde{a} \\ 0 & \tilde{b} & \tilde{a} & 0 \end{pmatrix} \quad (3.18)$$

The followings give the important experimental characteristics of a directional coupler

Coupling

Look at Fig(3.3), power is fed to port-1 and is measured at port-3 and the unused ports are terminated. Now the coupling C between port-1 and port-3 is defined as

$$C = 10 \log \frac{P_1}{P_3} \quad (3.19)$$

in decibels.

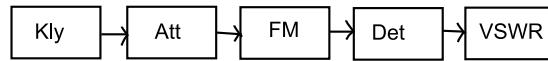


Figure 3.4: Measurement of incident power.

Directivity

Look at Fig(3.3), power is fed to port-1 and it has to be measured at port-4. If the directional coupler has only three ports and the fourth one is already terminated by a matched load then reverse the directional coupler so as to obtain port-4. Now measure the power at this port-4 and the power at port-3 is already measured in the above coupling section. Now the directivity D is defined as

$$D = 10 \log \frac{P_3}{P_4} \quad (3.20)$$

Isolation

Let P_1 be the incident power and P_4 be the power at the port-4 as measured in the above section. Isolation I is defined as

$$I = 10 \log \frac{P_1}{P_4} = C + D \quad (3.21)$$

3.3 Experimental procedure

Apparatus

Klystron, attenuator, frequency Meter, directional coupler, detector and VSWR meter.

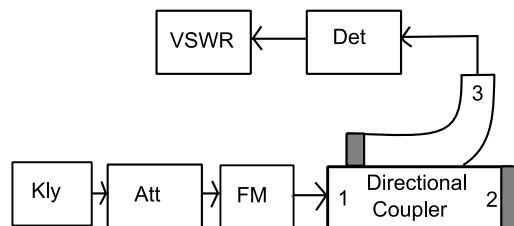


Figure 3.5: Power at Port-3

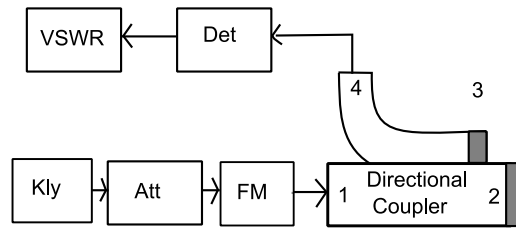


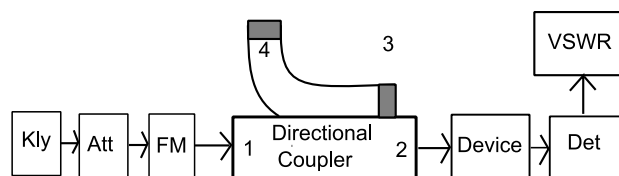
Figure 3.6: Power at Port-4.

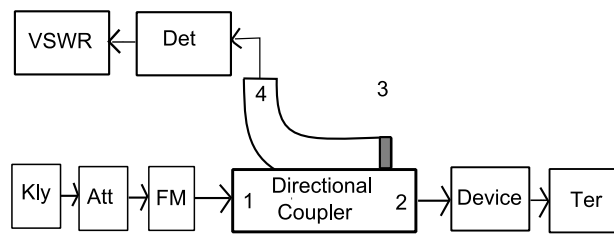
Measurement of coupling, directivity and isolation

1. Measure the incident power using the schematics in Fig.3.4. The power after FM is noted as P_1 and it will be used as an input to the directional coupler at port-1.
2. Measure the forward transmitted power P_3 using the schematics of Fig.3.5. Use Eq.(3.19) to calculate the coupling C .
3. Measure the forward transmitted power P_3 using the schematics of Fig.3.5. Also measure the backward transmitted power P_4 using the schematics of Fig.3.6. Calculate the directivity D using Eq.(3.20).
4. Use P_1 and P_4 measured as above and calculate the isolation I using Eq.(3.21).
5. Measure the power division by a dielectric load using block diagrams Fig.3.7 and Fig.3.8. Measure P_i like in Fig.3.7, without the device after the coupler. Measure P_t and P_r at ports 2 (now it is after the device) and 4, respectively. Estimate the power absorption using the conservation law given by

$$P_i = P_t + P_r + P_a, \quad (3.22)$$

where P_t , P_r and P_a give the transmitted, reflected and absorbed power, respectively in power units.

Figure 3.7: Measurement of transmitted power P_t .

Figure 3.8: Measurement of reflected power P_r .

6. Repeat the above steps for another power level.

NOTE: Eq3.22 can be written in the following form

$$1 = T + R + A \quad (3.23)$$

$$= \frac{P_t}{P_i} + \frac{P_r}{P_i} + \frac{P_a}{P_i} \quad (3.24)$$

$$= 10^{-(\bar{P}_t - \bar{P}_i)/10} + 10^{-(\bar{P}_r - \bar{P}_i)/10} + A \quad (3.25)$$

where quantities with over bars are power in dB. Substitute \bar{P}_i , \bar{P}_r and \bar{P}_t in the above equation to estimate A.

3.4 Conclusions

List out your main observations and conclusions.

Chapter 4

Magic Tee

4.1 Objectives

To measure the characteristics of the magic tee such as isolation and coupling

4.2 Theoretical background

In the previous section we discussed the theory of a general N-port junction. Here we present few other examples of such junctions, e.g., E -plane H -plane and magic tee.

4.2.1 E -plane tee

4.2.2 H -plane tee

4.2.3 Magic tee

Magic Tee is a four-port junction which is a combination of an E -plane tee and an H -plane tee (see Fig(4.1)). As shown in fig the collinear arms (arm 1 and arm 2) are called the side arms. The arm which makes an H -plane tee with the side arms is called the H -arm or *shunt arm*. The fourth arm makes an E -plane tee with the side arms and is thus the E -arm or *series arm*. The shunt and series arms are cross-polarized i.e., the voltage vectors in these two arms are perpendicular to each other. Therefore, as long as there is nothing within the junction to rotate the polarization, there can be no coupling between these two arms. The E -arm sees only the side arms and in fact these three ports behave like an E -plane tee. Similarly the H -arm and side arms together behave like an H -plane tee. The "magic" associated with this hybrid junction is the way that power divides in the

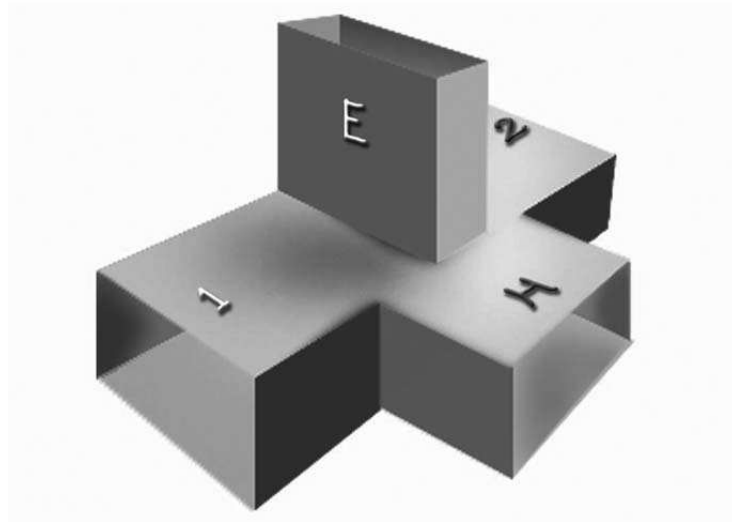


Figure 4.1: View of magic tee

various arms. If a signal is fed into the shunt or H-arm, power divides equally and *in phase* in the two side arms, with no coupling to the E-arm. When a signal enters the E-arm, it also divides equally in the two side arms, but this time the two halves are 180° out of phase, and there is no coupling to the H-arm. If power is fed into a side arm, it divides equally in to the shunt and series arms and there is no coupling to the collinear side arm.

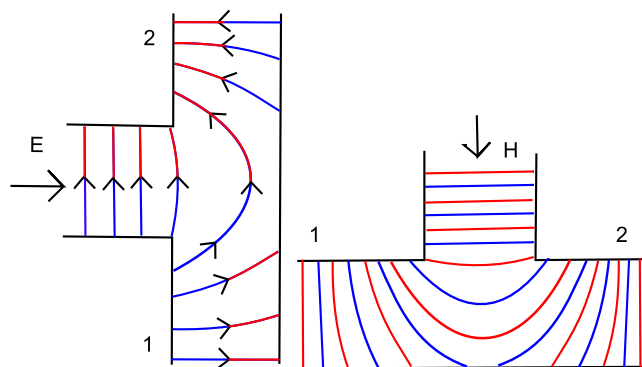


Figure 4.2: Phase distribution.

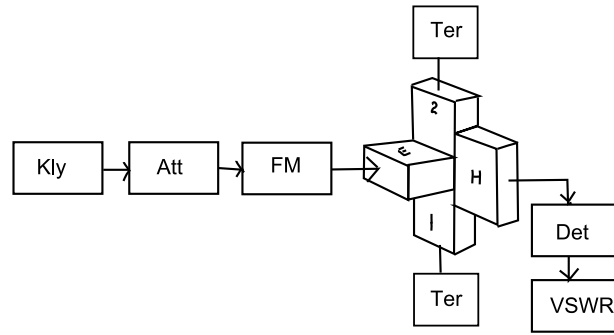


Figure 4.3: Isolation.

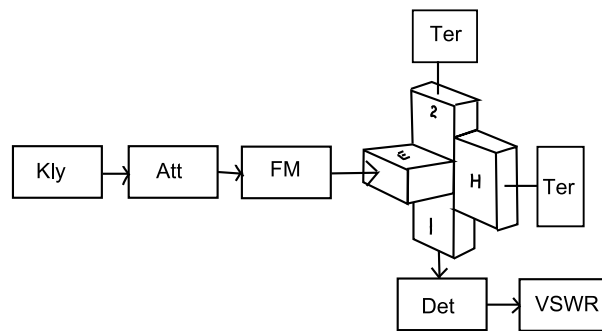


Figure 4.4: Coupling.

4.2.4 Isolation

Isolation can be calculated as

$$I_1 = 10 \log \frac{P_E}{P_H}, \text{ if the input is through } E - \text{ arm} \quad (4.1)$$

$$I_2 = 10 \log \frac{P_H}{P_E}, \text{ if the input is through } H - \text{ arm} \quad (4.2)$$

4.2.5 Coupling

$$C_1 = 10 \log \frac{P_E}{P_1} \text{ or } 10 \log \frac{P_E}{P_2}, \text{ if the input is through } E - \text{ arm} \quad (4.3)$$

$$C_2 = 10 \log \frac{P_H}{P_1} \text{ or } 10 \log \frac{P_H}{P_2}, \text{ if the input is through } H - \text{ arm} \quad (4.4)$$

4.3 Experimental procedure



Figure 4.5: Direct power.

Apparatus

Klystron, Attenuator, Frequency Meter, Magic Tee, Detector and VSWR meter.

Measurement of Isolation and Coupling

1. Measure the incident(direct) power using the schematics in Fig.4.5. The power after FM is noted as P_i and it will be used as an input to the magic tee.
2. Give the direct power to the E-arm and measure the power at H-arm using the schematics of Fig4.3. Use Eq.(4.1) to calculate the isolation I . Also calculate the isolation for the other case see Eq4.2.
3. Give the direct power to the E-arm and measure the power at the parallel arms(arm-1 or arm-2) see fig4.4. Use Eq4.3 to measure the coupling C . Measure the coupling between the H-arm and parallel arms also see Eq4.4.
4. Repeat the above steps for another power level.

Chapter 5

Klystron

To study and characterize the modes of a reflex klystron

5.1 Theoretical background

The two cavity or reflex klystrons are widely used in microwave technology for amplification and generation of microwave signals. Their principle of operation is similar except for the difference in the reflex klystron where the path of the electrons is reversed and the same cavity is used. The schematics of the two cavity klystron is shown in Fig.5.1. All electrons arriving from the cathode enter the first cavity with uniform velocity. At zeroes of the cavity gap voltage the electron velocity is not affected, while for the positive (negative) cycle the electrons get accelerated (decelerated). This results in a bunching of the electrons in their path (hence the first cavity is referred to as a buncher). The variation of the electron velocity in the drift space (between the cavities) is called the velocity modulation. The cavities used for Klystrons are referred to as the reentrant cavities (learn more about their construction and the principle of operation).

The electron density variation in the second cavity gap varies cyclically in time. The electron beam contains an AC component and is said to be current modulated. The maximum bunching should occur approximately midway between the grids of the second cavity during its retarding phase. The kinetic energy is then transferred from the electrons to the field of the second cavity and the electrons emerge with reduced velocity and get terminated at the collector.

In order to understand the velocity modulation and other processes, we need to make certain approximations. Keep in mind that the actual processes taking place in the cavities are too difficult to be treated by any quantitative theory. Nevertheless, the approximate analysis gives a fairly good idea about the relevant

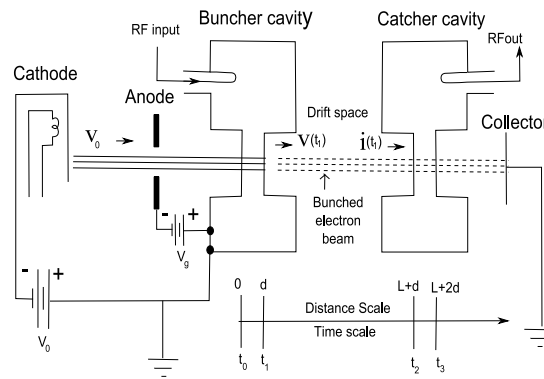


Figure 5.1: Two-cavity klystron.

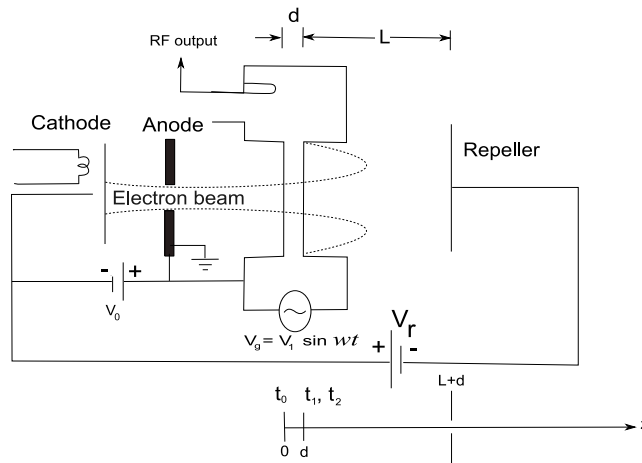


Figure 5.2: Reflex klystron.

processes.

1. Uniform density of the electron beam in any transverse plane. Transverse variations are ignored.
2. Space charge effects are ignored.
3. The magnitude of the microwave input is assumed to be much smaller than the dc accelerating voltage.

5.1.1 Velocity modulation

We assume that the electrons start at the cathode with null velocity. After getting accelerated, they achieve a uniform velocity v_0 at the entrance of the buncher grid given by

$$v_0 = \sqrt{\frac{2eV_0}{m}} = 0.593 \times 10^6 \sqrt{V_0} \text{ m/s} \quad (5.1)$$

Let a small microwave signal $V_s = V_1 \sin(\omega t)$ be applied to the input terminal, so that $V_1 \ll V_0$. The average transit time through the buncher gap d is

$$\tau \sim \frac{d}{v_0} = t_1 - t_0 \quad (5.2)$$

The average gap transit angle is then given by

$$\theta_g = \omega\tau = \omega(t_1 - t_0) = \frac{\omega d}{v_0}. \quad (5.3)$$

The average microwave voltage in the buncher gap can be expressed as

$$\begin{aligned} \langle V_s \rangle &= \frac{1}{\tau} \int_{t_0}^{t_1} V_1 \sin(\omega t) dt \\ &= -\frac{V_1}{\omega\tau} [\cos(\omega t_1) - \cos(\omega t_0)] \\ &= \frac{V_1}{\omega\tau} [\cos(\omega t_0) - \cos(\omega t_0 + \frac{\omega d}{v_0})] \end{aligned} \quad (5.4)$$

The above equation can be written in the form

$$\begin{aligned} \langle V_s \rangle &= V_1 \frac{\sin[\omega d/2v_0]}{\omega d/2v_0} \sin(\omega t_0 + \frac{\omega d}{2v_0}) \\ &= V_1 \frac{\sin[\theta_g/2]}{\theta_g/2} \sin(\omega t_0 + \frac{\theta_g}{2}) \end{aligned} \quad (5.5)$$

We have introduced the beam coupling coefficient β_i as

$$\beta_i = \frac{\sin[\omega d/2v_0]}{\omega d/2v_0} = \frac{\sin[\theta_g/2]}{\theta_g/2}. \quad (5.6)$$

As can be easily seen from this equation that the beam coupling decreases rapidly with an increase in the gap transit angle. After velocity modulation the exit velocity from the buncher gap is then given by

$$\begin{aligned} v(t_1) &= \sqrt{\frac{2e}{m} \left[V_0 + \beta_i V_1 \sin(\omega t_0 + \frac{\theta_g}{2}) \right]} \\ &= \sqrt{\frac{2e}{m} V_0 \left[1 + \frac{\beta_i V_1}{V_0} \sin(\omega t_0 + \frac{\theta_g}{2}) \right]} \end{aligned} \quad (5.7)$$

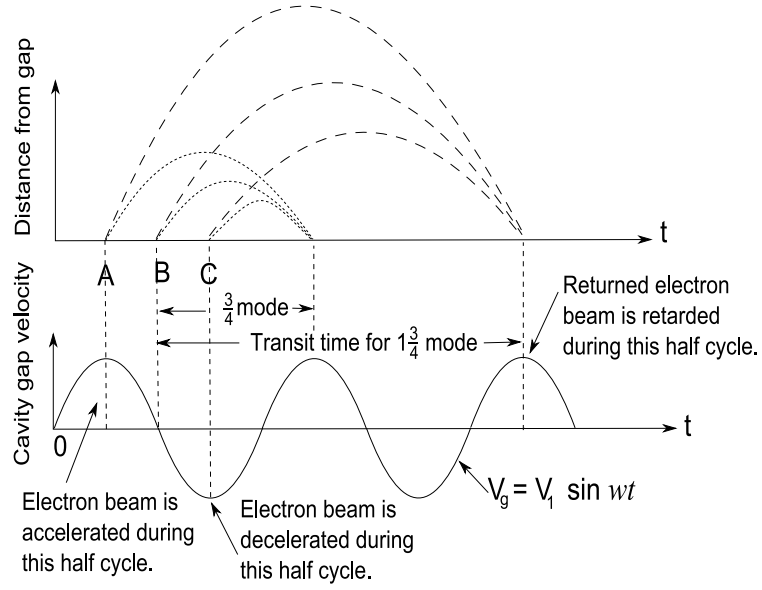


Figure 5.3: Bunching process and the origin of various modes.

Here the factor $\beta_i V_1 / V_0$ is called the depth of velocity modulation. Under the approximation of small depth of modulation $\beta_i V_1 \ll V_0$, this equation can be approximated by

$$v(t_1) = v_0 \left[1 + \frac{\beta_i V_1}{2V_0} \sin(\omega t_0 + \frac{\theta_g}{2}) \right] = v_0 \left[1 + \frac{\beta_i V_1}{2V_0} \sin(\omega t_1 - \frac{\theta_g}{2}) \right] \quad (5.8)$$

Up to this point the theory of a two-cavity and reflex klystron is the same. Henceforth we will concentrate only on the reflex klystron (see figure). After the cavity the velocity modulated electrons enter the repeller region. All electrons turned around by the repeller then pass through the cavity gap in bunches. On their journey the bunched electrons pass through the gap during the retarding phase of the alternating field and give up their kinetic energy to the cavity field. Oscillator output energy is then taken from the cavity. After their job is over, the electrons are collected by the cavity walls or other grounded metal parts of the tube. The velocity modulated electron is forced back to $z = d$ of the cavity by the retarding electric field E given by

$$E = \frac{V_r + V_0 + V_1 \sin(\omega t)}{L} \quad (5.9)$$

Neglecting the small oscillatory component, one can write down the equation of motion for the electron in the repeller region as

$$m \frac{d^2 z}{dt^2} = -eE = -e \frac{V_r + V_0}{L} \quad (5.10)$$

Integrating in the interval from t_1 to t , we have

$$\frac{dz}{dt} = -e \frac{V_r + V_0}{L} \int_{t_1}^t dt = \frac{-e(V_r + V_0)}{mL} (t - t_1) + K_1 \quad (5.11)$$

At $t = t_1$, $dz/dt = v(t_1) = K_1$. Hence

$$z = -e \frac{V_r + V_0}{2mL} (t - t_1)^2 + v(t_1)(t - t_1) + d \quad (5.12)$$

Here we used the fact that at $t = t_1$, $z = d$. Assuming that the electron leaves the gap at $z = d$ at $t = t_1$ with a velocity of $v(t_1)$ and returns to the same location $z = d$ at $t = t_2$, we have

$$0 = -e \frac{V_r + V_0}{2mL} (t_2 - t_1)^2 + v(t_1)(t_2 - t_1) \quad (5.13)$$

Thus the round trip transit time is given by

$$T' = t_2 - t_1 = \frac{2mL}{e(V_0 + V_r)} v(t_1) = T'_0 \left[1 + \frac{\beta_i V_1}{2V_0} \sin(\omega t_1 - \frac{\theta_g}{2}) \right], \quad (5.14)$$

where the dc roundtrip transit time T'_0 is given by

$$T'_0 = \frac{2mLv_0}{e(V_0 + V_r)} \quad (5.15)$$

The corresponding phase angle is given by

$$\omega(t_2 - t_1) = \theta'_0 + X' \sin(\omega t_1 - \theta_g/2), \quad \theta'_0 = \omega T'_0, \quad X' = \frac{\beta_i V_1}{2V_0} \theta'_0 \quad (5.16)$$

where θ'_0 is the round trip dc transit angle and X' is the bunching parameter.

5.1.2 Power output and efficiency

In order to generate maximum power, the returning electron beam must cross the cavity gap when the gap field is maximum retarding. This is the way the electrons can impart maximum kinetic energy to the field. It can be seen from the fig. that for maximum energy transfer, the round trip transit angle, referring to the center of the bunch, must be given by

$$\omega(t_2 - t_1) = \theta'_0 = 2\pi \left(n - \frac{1}{4} \right) = 2\pi N = 2\pi n - \frac{\pi}{2}, \quad (5.17)$$

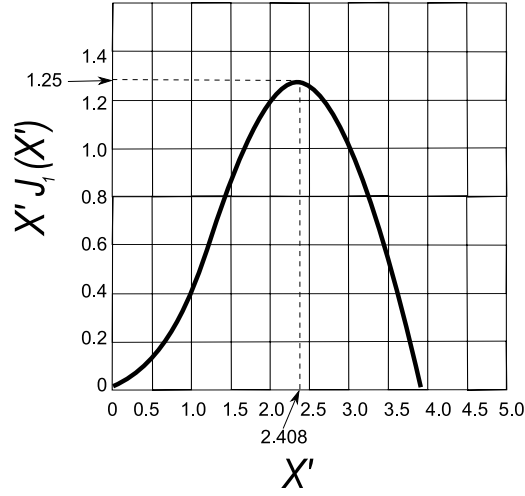


Figure 5.4: $X' J_1(X')$ as a function of X' .

where n is any positive integer and $N = n - 1/4$ is the number of the mode. The beam current of a reflex klystron can be written as

$$i_{2t} = -I_0 - \sum_{n=1}^{\infty} 2I_0 J_n(nX') \cos[n(\omega t_2 - \theta'_0 - \theta_g)] \quad (5.18)$$

The fundamental component of the induced current is given by

$$i_2 = -\beta_i i_{2f} = 2\beta_i I_0 J_1(X') \cos(\omega t_2 - \theta'_0), \quad (5.19)$$

where the magnitude $I_2 = 2\beta_i I_0 J_1(X')$ and we neglected θ_g . The dc power supplied by the voltage V_0 is

$$P_{dc} = V_0 I_0 \quad (5.20)$$

and the ac power is given by

$$P_{ac} = \frac{V_1 I_2}{2} = \beta_i I_0 J_1(X') \quad (5.21)$$

Using Eqs. (5.16) and (5.17) one has

$$\frac{V_1}{V_0} = \frac{2X'}{\beta_i(2\pi n - \pi/2)}, \quad (5.22)$$

which leads to the final expression for P_{ac} as

$$P_{ac} = \frac{2V_0 I_0 X' J_1(X')}{(2\pi n - \pi/2)} \quad (5.23)$$

One can define the efficiency of the klystron η as

$$\eta = \frac{P_{ac}}{P_{dc}} = \frac{2X'J_1(X')}{(2\pi n - \pi/2)} \quad (5.24)$$

The factor $X'J_1(X')$ attains a maximum value 1.25 at $X' = 2.408$ with $J_1(2.408) = 0.52$. Generally the mode with $n = 2$ has the maximum power. For that mode one has

$$\eta = \frac{2 \times 2.408 \times 0.52}{(2\pi \times 2 - \pi/2)} = 22.7\% \quad (5.25)$$

Substituting Eqs.(5.1) and (5.17) in Eq.(5.15), one can find the relation between the repeller voltage and the cycle number n

$$\frac{V_0}{(V_0 + V_r)^2} = \frac{e(2\pi n - \pi/2)^2}{8m\omega^2 L^2} \quad (5.26)$$

P_{ac} can also be expressed in terms of the repeller voltage as

$$P_{ac} = \frac{V_0 I_0 X' J_1(X') (V_r + V_0)}{\omega L} \sqrt{\frac{e}{2mV_0}} \quad (5.27)$$

Eq.(5.26) implies that for a given beam voltage V_0 and cycle number n the center repeller voltage can be determined in terms of the center frequency. Then the power output at the center frequency can be calculated using Eq.(5.27). When the frequency varies from the center frequency and the repeller voltage about the center repeller voltage, the power output will vary accordingly assuming a bell shape (see Fig.).

5.2 Apparatus and measurements

Klystron Power Supply, Klystron, Attenuator, Frequency Meter, Detector, VSWR meter and Oscilloscope

5.2.1 Experimental setup with VSWR

Experimental steps

1. Set V_0 at some constant voltage.
2. Vary V_R and find the frequency from FM, amplitude from VSWR for different values of V_R
3. Plot VSWR and FM readings against V_R readings

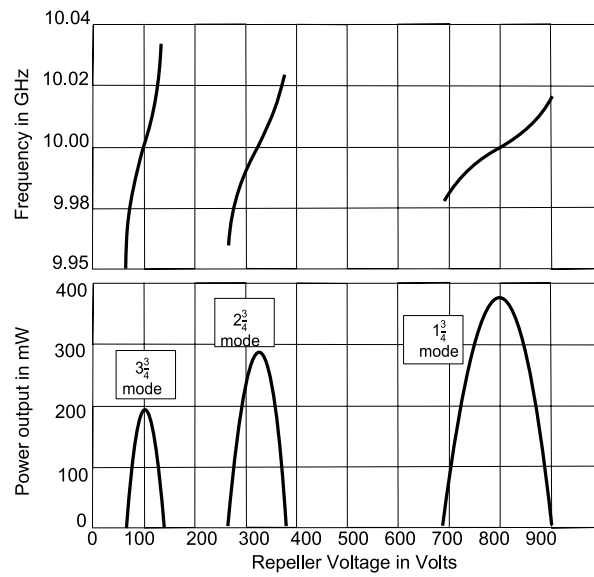


Figure 5.5: Klystron frequency and power as functions of the repeller voltage V_r .

5.2.2 Experimental setup with Oscilloscope:

Experimental steps

1. Modulate the V_R amplitude with a linear ramp voltage
2. Connect the modulated V_R to the XX terminal of CRO and YY terminals to the Detector
3. Observe the modes displayed by the CRO and record the amplitudes and frequencies of the modes

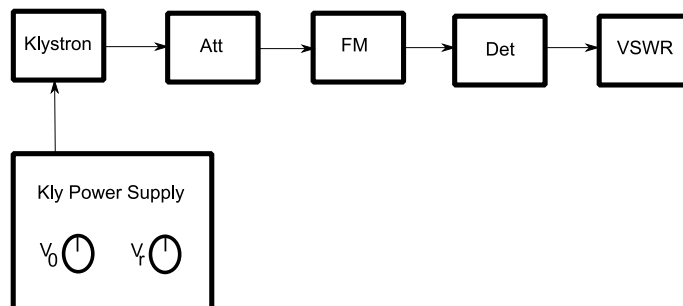


Figure 5.6: block diagram.

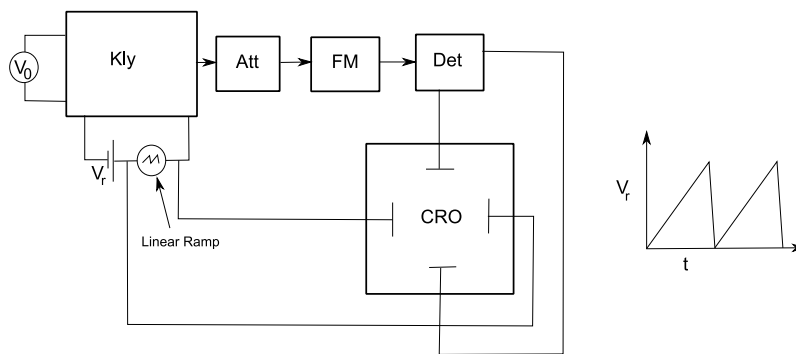


Figure 5.7: block diagram.

5.2.3 Data collection and analysis

Setup with VSWR

Sl.No	V_R	VSWR	FM
1			
2			
3			

Setup with CRO

	V_1, V_2, V_3, V_4, V_5	$V_{r1}, V_{r2}, V_{r3}, V_{r4}, V_{r5}$	f_1, f_2, f_3, f_4, f_5
Mode1			
Mode2			
Mode3			

5.3 Conclusions

- 1.
- 2.
- 3.

NOTE: Items 5.2.3 and 5.3 are to be submitted as the Lab Experiment Report

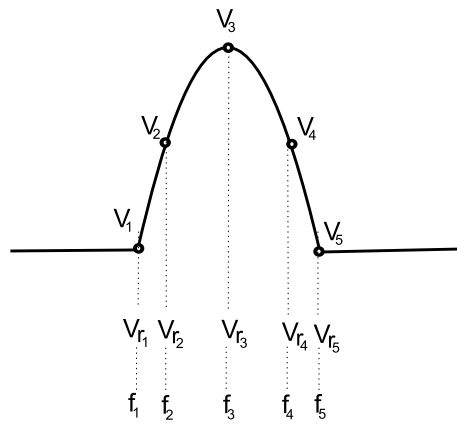


Figure 5.8: block diagram.

Chapter 6

Gunn Diode

6.1 Objectives

1. V-I Characteristics
2. Output Power and frequency as a function of Bias voltage
3. Mechanical Tuning of Output Power and frequency
4. Square wave modulation through PIN diode

6.2 Theoretical background

6.2.1 The Gunn Effect

In some materials (III-V compounds such as GaAs and InP), after an electric field in the material reaches a threshold level, the mobility of electrons decrease as the electric field is increased, thereby producing negative resistance. A two-terminal device made from such a material can produce microwave oscillations, the frequency of which is primarily determined by the characteristics of the specimen of the material and not by any external circuit. The Gunn Effect was discovered by J. B. Gunn of IBM in 1963.

6.2.2 The Gunn Diode

In certain semiconductors, notably GaAs, electrons can exist in a high-mass low velocity state as well as their normal low-mass high-velocity state and they can be forced into the high-mass state by a steady electric field of sufficient strength. In this state they form clusters or domains which cross the field at a constant rate

causing current to flow as a series of pulses. This is the Gunn effect and one form of diode which makes use of it consists of an epitaxial layer of n-type GaAs grown on a GaAs substrate. A potential of a few volts applied between ohmic contacts to the n-layer and substrate produces the electric field which causes clusters. The frequency of the current pulses so generated depends on the transit time through the n-layer and hence on its thickness. If the diode is mounted in a suitably tuned cavity resonator, the current pulses cause oscillation by shock excitation and r.f. power up to 1 W at frequencies between 10 and 30 GHz is obtainable.

Gunn Oscillator:

In a Gunn Oscillator, the Gunn Diode is placed in a resonant cavity. In this case the oscillation frequency is determined by cavity dimension than by the diode itself. Although Gun Oscillator can be amplitude-modulated with the bias v

Usually the Gunn diode is mounted on a post structure between the waveguide walls, either $l g/2$ from an iris or $l g/2$ from a short circuit (see Figure6.1). Some alteration is necessary to set the exact frequency to allow for diode and package parasitics and manufacturing tolerances. Tuning screws (either metal or dielectric) are used to modify the cavity resonant frequency. Power output variations are achieved by adjusting the coupling between diode and load using variations in post size or tuning screws as shown in Figure6.1

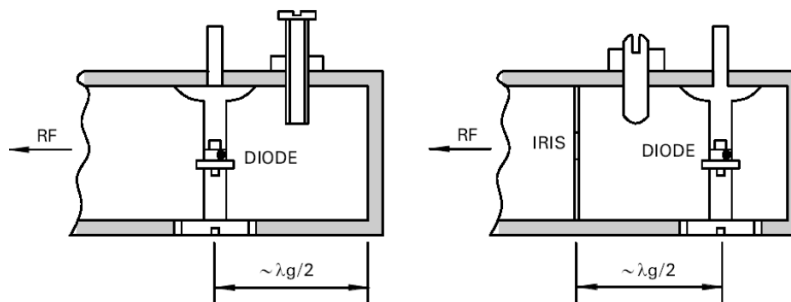


Figure 6.1: Mechanical Tuning

6.2.3 Theory

The Gunn diode is a so-called transferred electron device. Electrons are transferred from one valley in the conduction band to another valley. In order to understand the nature of the transferred electron effect exhibited by Gunn diodes, it is necessary to consider the electron drift velocity versus electric field (or current versus voltage) relationship for GaAs (see Figure 6.2). Below the threshold field, E_{th} , of approximately 0.32 V/mm, the device acts as a passive resistance. However, above E_{th} the electron velocity (current) decreases as the field (voltage) increases producing a region of negative differential mobility, NDM (resistance, NDR). This is the essential feature that leads to current instabilities and Gunn oscillations in an active device and is due to the special conduction band structure of direct band gap semiconductors such as GaAs (see Figure 6.3).

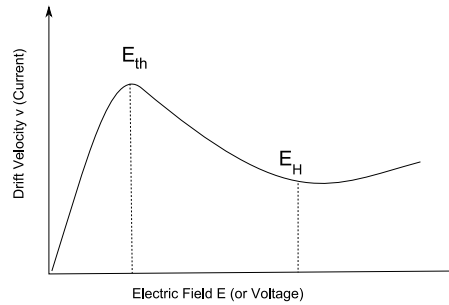


Figure 6.2: Negative Resistive Region

The energy-momentum relationship contains two conduction band energy levels, Γ and L (also known as valleys) with the following properties:

1. In the lower Γ valley, electrons exhibit a small effective mass and very high mobility, μ_1 .
2. In the satellite L valley, electrons exhibit a large effective mass and very low mobility, μ_2 .
3. The two valleys are separated by a small energy gap, ΔE , of approximately 0.31 eV.

In equilibrium at room temperature most electrons reside near the bottom of the lower Γ valley. Because of their high mobility ($8000 \text{ cm}^2 \text{ V}^{-1} \text{ s}^{-1}$), they can readily be accelerated in a strong electric field to energies in the order of the Γ -L intervalley separation, ΔE . Electrons are then able to scatter into the satellite L valley, resulting in a decrease in the average electron mobility, μ_1 , as given below:

$$\mu = (n_1 \mu_1 + n_2 \mu_2) / (n_1 + n_2) \quad (6.1)$$

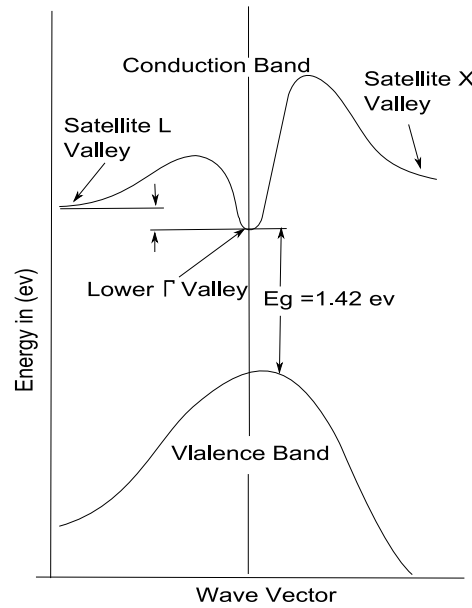


Figure 6.3: Two Valley Model

where n_1 = electron density in Γ valley, n_2 = electron density in L valley

Above the high field, E_H , most electrons reside in the L valley and the device behaves as a passive resistance (of greater magnitude) once again.

In a practical Gunn diode, electrons are accelerated from the cathode by the prevailing electric field. When they have acquired sufficient energy, they begin to scatter into the low mobility satellite valley and slow down.

The question of exactly how the NDR phenomenon in GaAs results in Gunn-oscillations can now be answered with the aid of Figure 6.4. A sample of uniformly doped n-type GaAs of length L is biased with a constant voltage source V_0 . The electrical field is therefore constant and its magnitude given by $E_0 = V_0/L$. From the bottom graph in Figure 6.4 it is clear that the electrons flow from cathode to anode with constant velocity v_3 .

It is now assumed that a small local perturbation in the net charge arises at $t = t_0$, indicated by the solid curve in Figure 6.4. This non-uniformity can, for example, be the result of local thermal drift of electrons. The resulting electrical field distribution is also shown (solid curve). The electrons at point A, experiencing an electric field EL_1 ,

will now travel to the anode with velocity v_4 . The electrons at point B is subjected to an electrical field EH_1 . They will therefore drift towards the anode with velocity v_2 which is smaller than v_4 . Consequently, a pile-up of electrons will occur between A and B, increasing the net negative charge in that region.

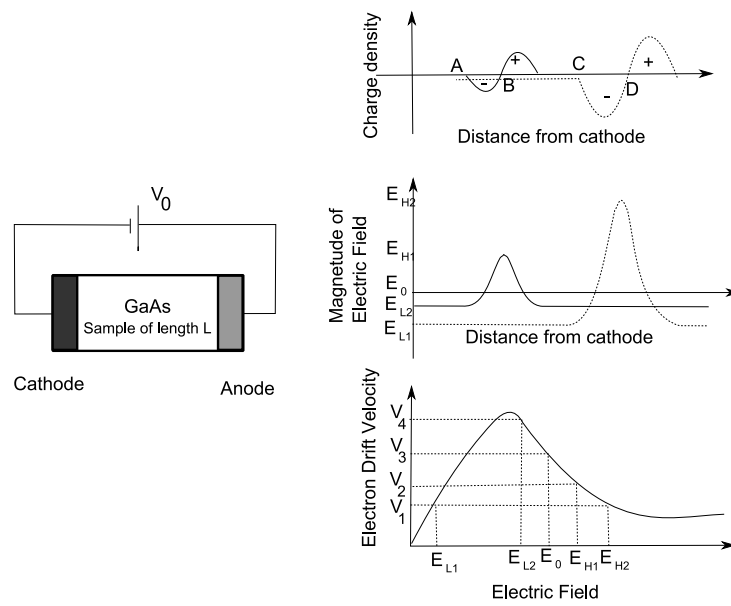


Figure 6.4:

The region immediately to the right of B will become progressively more depleted of electrons, due to their higher drift velocity towards the anode than those at B. The initial charge perturbation will therefore grow into a dipole domain, commonly known as a Gunn-domain. Gunn domains will grow while propagating towards the anode until a stable domain has been formed. A stable Gunn-domain is shown at a time instance $t > t_0$, indicated by the dashed curve. At this point in time, the domain has grown sufficiently to ensure that electrons at both points C and D move at the same velocity, v_1 , as is clear from the bottom graph in Figure 6.4. It is important to note that the sample had to be biased in the NDR region to produce a Gunn-domain. Once a domain has formed, the electric field in the rest of the sample falls below the NDR region and will therefore inhibit the formation of a second Gunn-domain. As soon as the domain is absorbed by the anode contact region, the average electric field in the sample rises and domain formation can again take place. The successive formation and drift of Gunn-domains through the sample leads to a.c. current oscillations observed at the contacts.

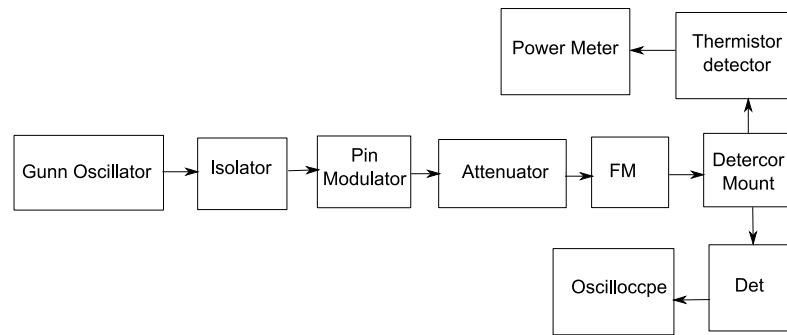


Figure 6.5:

6.3 Experimental Setup

6.3.1 Apparatus Required

Gunn oscillator, Gunn power supply, PIN modulator, Isolator, Frequency meter, Variable attenuator, Detector, VSWR meter, Cables and Accessories.

6.3.2 Experimental Procedure

1. Set the components and equipments as shown in the Fig6.5.
2. Initially set the variable attenuator for maximum attenuation
3. Switch off the control knob and keep low the all other knob of the Gunn Power
4. Set the micrometer of Gunn Oscillator for required frequency of operation.
5. Switch ON the Cooling fan before switching on the Gunn Power Supply.

6.3.3 Voltage-current characteristics

1. Turn the meter switch of Gunn power supply to voltage position.
2. Increase the Gunn diode bias voltage in steps and measure the Gunn diode current in each step. Do not exceed the bias voltage above 10 volts.
3. Plot the voltage and current readings on the graph as shown in Fig6.6(left).
4. Measure the threshold voltage which corresponds to maximum current.

6.3.4 Output power and frequency as function of Gunn bias voltage

1. Turn the meter switch of Gunn power supply to voltage position.
2. Increase the Gunn bias voltage control knob.
3. Rotate PIN bias knob to around maximum position.
4. Measure the frequency by frequency meter and detune it before measuring the power.
5. Measure the power from power meter which is connected through a thermistor detector corresponding to the various bias voltage.
6. Use the reading to draw the power vs Voltage curve and frequency vs voltage and plot the graph.
7. Measure the frequency sensitivity against variation in bias voltage.

6.3.5 Mechanical Tuning of Output Power and frequency

1. Set the Gunn bias voltage in NDR region (above V_{th})
2. Turn the Tuning Screw of The Gunn Oscillator in step of mm
3. Measure the frequency by FM and detune it before measuring the power
4. Measure also the power from power meter corresponding to the various positions of the Tuning screw.
5. Plot a curve for Power and Frequency against Tuning screw readings
6. Observe the range and sensitivity of the mechanical tuning from the graphs.

6.3.6 Square wave modulation through PIN diode

1. Keep the meter switch of Gunn Power Supply to volt position and set Gunn bias voltage slowly above V_{th} .
2. Tune the PIN modulator bias voltage and frequency knob for maximum output on the oscilloscope.
3. Coincide the bottom of square wave in oscilloscope to some reference level and note down the micrometer reading of variable attenuator.

4. Now with the help of variable attenuator coincide the top of square wave to same reference level and note down the micrometer reading.
5. Connect VSWR to detector mount and note down the db reading in VSWR meter for both the micrometer reading of the variable attenuator.
6. The difference of both db reading of VSWR meter gives the modulation depth of PIN modulator.

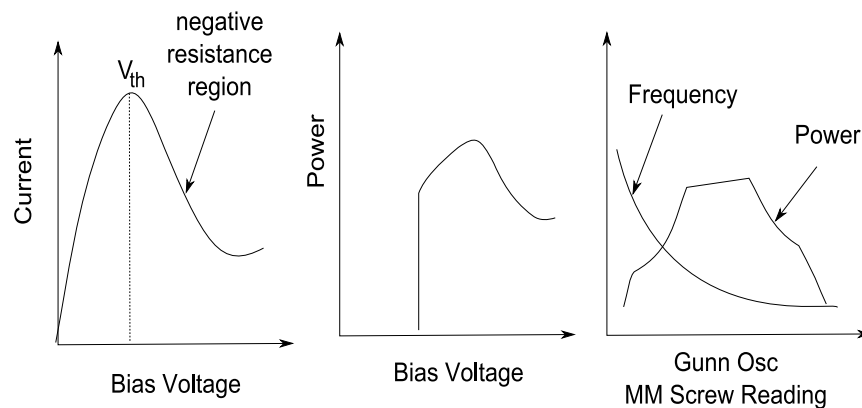


Figure 6.6:

Note

1. Isolator must be used between the Gunn Oscillator and the PIN Modulator
2. donot keep gunn bias knob position at threshold position for more than 10-15 seconds. reading should be obtained as fast as possible. otherwise, due to excessive heating, gunn diode may burn.

Acknowledgement

In preparing the theoretical portion we used extensively the material available at
<http://www.nhn.ou.edu/~johnson/Education/Juniorlab/Microwave/Gunn%20Effect.pdf>
<http://www.rfglobalnet.com/article.mvc/Introduction-To-Gunn-Diodes-0001>

Chapter 7

Horn Antenna

7.1 Objectives

To estimate the Gain, radiation field pattern and 3-dB beam width for E-plane and H-planes of the horn antenna.

7.2 Introduction

It is an open-ended waveguide, of increasing cross-sectional area, which radiates directly in a desired direction or feeds a reflector that forms a desired beam.

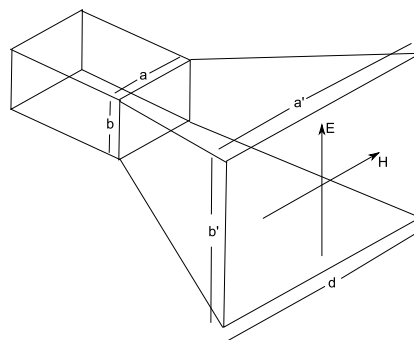


Figure 7.1: Horn Antenna.

Linearly polarized waves are radiated by a waveguide horn antenna, the direction of polarization being parallel to the narrow dimension of the waveguide feeding the antenna. The reason is that the waveguide field has only one electric field component parallel to the narrow wall of the guide. Because of this and by virtue of the principle of reciprocity such a horn can only receive waves of the

same polarization as that it radiates, and so if the incident field is arbitrarily polarized the horn selects the components of the field aligned with its direction of polarization. If the only field component is perpendicular to the horn's direction of polarization, then the horn does not receive the incident field.

Basic horn antenna concept

The horn antenna may be considered as an RF transformer or impedance match between the waveguide feeder and free space which has an impedance of 377 ohms. By having a tapered or having a flared end to the waveguide the horn antenna is formed and this enables the impedance to be matched. Although the waveguide will radiate without a horn antenna, this provides a far more efficient match.

In addition to the improved match provided by the horn antenna, it also helps suppress signals traveling via unwanted modes in the waveguide from being radiated.

However the main advantage of the horn antenna is that it provides a significant level of directivity and gain. For greater levels of gain the horn antenna should have a large aperture. Also to achieve the maximum gain for a given aperture size, the taper should be long so that the phase of the wave-front is as nearly constant as possible across the aperture. However there comes a point where to provide even small increases in gain, the increase in length becomes too large to make it sensible. Thus gain levels are a balance between aperture size and length. However gain levels for a horn antenna may be up to 20 dB in some instances.

7.3 Experimental setup

7.3.1 Apparatus required

Klystron, Isolator, Frequency meter, Attenuator, Waveguide stands, two horn antennas, 90°twister, rotatable stand calibrated in degrees(protractor), Detector and VSWR meter.

7.4 Gain

7.4.1 Gain of the Horn antenna for E and H planes

1. Keep the transmitting and receiving Horn antennas in the same line such that one faces the other as shown in fig7.2.
2. Keep the antennas with a distance(R) between them $\geq 2D^2/\lambda_0$

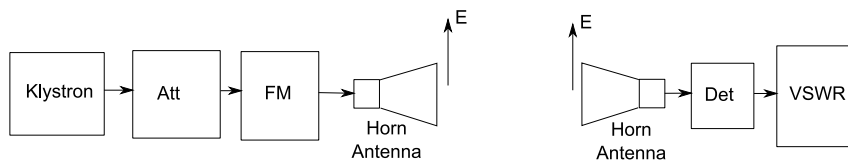


Figure 7.2: Gain when H-field is parallel to ground.

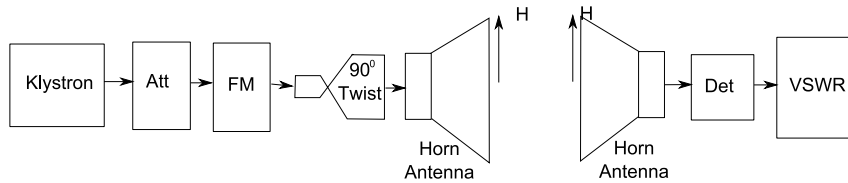


Figure 7.3: Gain when E-field is parallel to ground

3. The two antennas must be aligned in similar polarization
4. Adjust the VSWR knobs and the attenuator(at the source) to get a VSWR reading as large as possible. Record it as P_r in dB.
5. Now remove the transmitting horn antenna and connect the detector to measure the direct power which should be noted as P_t in db.
6. Get the ratio in mw and estimate gain G

$$10 \log \frac{P_r}{P_t} = P_r \text{ in dB} - P_t \text{ in dB}$$

$$\Rightarrow \frac{P_r}{P_t} = 10^{(P_r \text{ in dB} - P_t \text{ in dB})/10} \quad (7.1)$$

$$G = \frac{4\pi R}{\lambda_0} \sqrt{\frac{P_r}{P_t}} \quad (7.2)$$

7. Use the above steps to estimate the gain for E-plane(E-field is parallel to the ground)
8. Use a 90° twist (see fig7.3) to rotate the transmitter such that H-field comes parallel to the ground. And measure the gain by keeping the receiver also in H-plane.

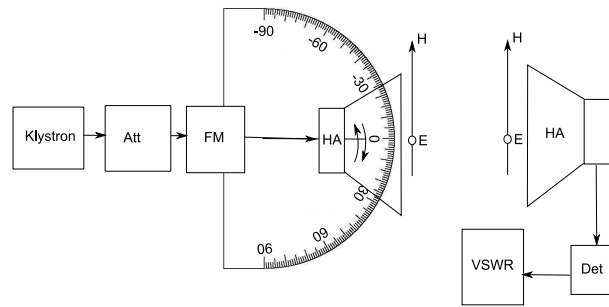


Figure 7.4: Field pattern when H-field is parallel to ground.

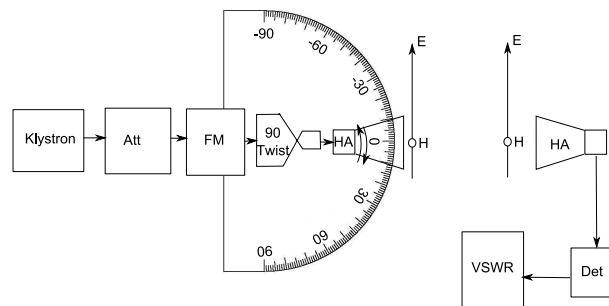


Figure 7.5: Field pattern when E-field is parallel to ground

7.5 Radiation field pattern for E and H planes

1. Keep the transmitting and receiving Horn antennas in the same line such that transmitter positioned at 0^0 on the rotating platform as shown in fig7.4.
2. Both antennas must be aligned in similar polarization.
3. The minimum distance(R) between the antennas should be $\geq 2D^2/\lambda_0$ to satisfy the far field pattern(Franhofer pattern)
4. Adjust the VSWR knobs and the attenuator(at the source) to get a VSWR reading as large as possible.
5. Record the VSWR readings at the receiving end corresponding to the different angular positions of the transmitter(Rotate the transmitter in steps of 10^0 and cover the full range from -90^0 to 90^0).
6. Repeat the above steps for E-plane and for H-plane

7. Plot these values to show the radiation field pattern see fig7.6. for both the planes

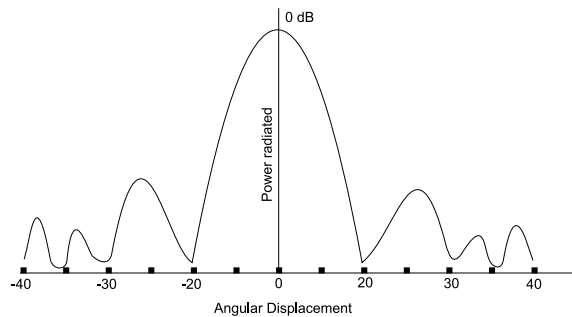


Figure 7.6: Radiation Field pattern

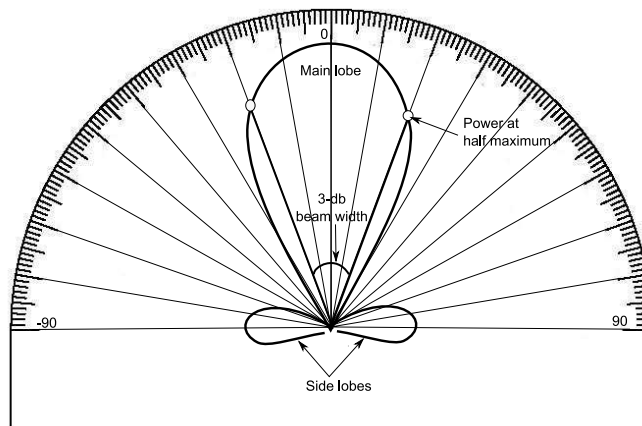


Figure 7.7: 3-dB beam width

7.6 3-dB Beam width

1. Use the above observations and plot the VSWR readings corresponding to the different angular positions of the horn antenna on a polar graph see fig7.7.
2. 3-dB beam width is the angle subtended by the points of half maximum power on the main lobe, see fig
3. Measure it for both E and H planes.

7.6.1 Acknowledgement

Introduction

[http://en.wikipedia.org/wiki/Horn_\(telecommunications\)](http://en.wikipedia.org/wiki/Horn_(telecommunications))

<http://faculty.kfupm.edu.sa/ee/ajmal/0xx/ee340new/EE340LabExperiment8.pdf>

Basic Horn antenna concept

http://www.radio-electronics.com/info/antennas/horn_antenna/horn_antenna.php

Chapter 8

Dielectric constant of solids

8.1 Objective

To measure the dielectric constant ϵ of solids using Von Hippel's method

8.2 Theoretical background

The dielectric behavior of materials at microwave frequencies can give information about the usage and application of the material at these frequencies. The principle of the terminated waveguide method (Von Hippel's Method) is shown schematically in Fig.8.1. The sample of thickness d fills the end section of a waveguide termi-

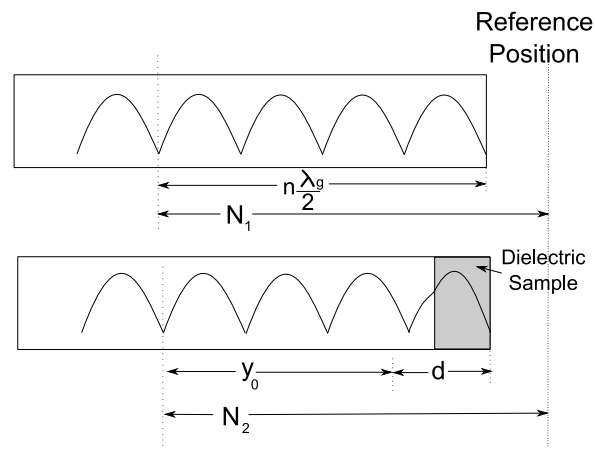


Figure 8.1: PRINCIPLE OF THE TERMINATED WAVEGUIDE METHOD.

nated by a short circuit. A slotted section of the guide interposed between the

sample and the generator makes it possible to determine the position of the first minimum (y_0) and the relative amplitude $r = \frac{E_{min}}{E_{max}}$ of the maxima and minima by means of a traveling detector probe. Because there is a length of waveguide intervening between the slotted section and the sample, and the scale on the probe reads from an arbitrary origin, the position of the first minimum must be found by taking a reference reading of the minimum in the absence of sample.

If the position of the minimum in the absence of sample is read on the scale of the slotted section at N_1

$$N_1 = n \frac{\lambda_g}{2} \quad (8.1)$$

where n is an integer.

If N_2 is the position of the minimum in the presence of the sample then:

$$N_2 = d + y_0 \quad (8.2)$$

from Eq.8.1 and Eq.8.2, we get

$$y_0 = N_2 - N_1 + n \frac{\lambda_g}{2} - d \quad (8.3)$$

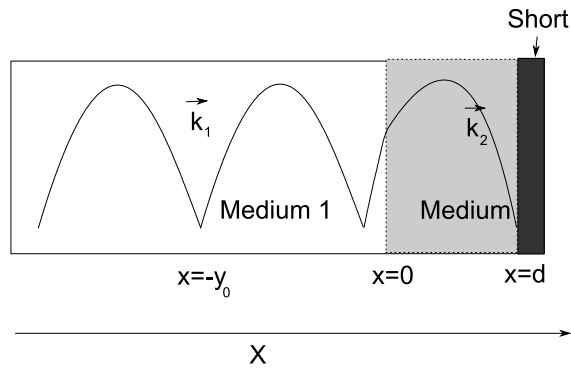


Figure 8.2:

Consider an EM wave traveling through medium 1 (air) strikes normally to the medium 2 (dielectric), a part of it is reflected and the rest gets transmitted see Fig.8.2. A standing wave pattern is thus produced in medium 1. The transverse electric field component in this partial reflection case is given by

$$E_1 = A_+ e^{jk_1 x} + A_- e^{-jk_1 x} \quad \text{in medium 1} \quad (8.4)$$

$$E_2 = B_+ e^{jk_2 x} + B_- e^{-jk_2 x} \quad \text{in medium 2} \quad (8.5)$$

where $k_1 = \frac{2\pi}{\lambda_g}$ and $k_2 = \frac{2\pi}{\lambda_{gd}}$ are the wave vectors in medium 1 and medium 2 (λ_g is guide wavelength in air and λ_{gd} is guide wavelength in dielectric)

Applying Boundary condition at the interface (at $x=0$), we have $E_1|_{x=0} = E_2|_{x=0}$ gives

$$A_+ + A_- = B_+ + B_- \quad (8.6)$$

and $\frac{dE_1}{dx}|_{x=0} = \frac{dE_2}{dx}|_{x=0}$ gives

$$k_1(A_+ - A_-) = k_2(B_+ + B_-) \quad (8.7)$$

Since waveguide is shorted at $x = d$, $E_2|_{x=d} = 0$. It gives

$$B_+ e^{jk_2 d} + B_- e^{-jk_2 d} = 0 \quad (8.8)$$

As y_0 is the position of a minima from the interface, electric field at this point ($x = -y_0$) must be zero. So we get

$$A_+ e^{-jk_1 y_0} + A_- e^{jk_1 y_0} = 0 \quad (8.9)$$

Eliminating A_+ , A_- and B_+ , B_- from the above equations 8.6, 8.7, 8.8 and 8.9, we get Eq.8.8 and Eq.8.9 in the above equation, we get

$$\begin{aligned} e^{2jk_1 y_0} &= \frac{(k_1 + k_2)e^{-2jk_2 d} - (k_1 - k_2)}{-(k_1 - k_2)e^{-2jk_2 d} + (k_1 + k_2)} \\ &= \frac{k_2(1 + e^{-2jk_2 d}) - k_1(1 - e^{-2jk_2 d})}{k_2(1 + e^{-2jk_2 d}) + k_1(1 - e^{-2jk_2 d})} \end{aligned} \quad (8.10)$$

rearranging, we get

$$\begin{aligned} \text{or } \frac{1 - e^{2jk_1 y_0}}{1 + e^{2jk_1 y_0}} &= \frac{k_1(1 - e^{-2jk_2 d})}{k_2(1 + e^{-2jk_2 d})} \\ \frac{(e^{-jk_1 y_0} - e^{jk_1 y_0})}{k_1(e^{-jk_1 y_0} + e^{jk_1 y_0})} &= \frac{(e^{jk_2 d} - e^{-jk_2 d})}{k_2(e^{jk_2 d} + e^{-jk_2 d})} \\ -\frac{\tan(k_1 y_0)}{k_1} &= \frac{\tan(k_2 d)}{k_2} \\ \text{or } \frac{\tan x}{x} &= -\frac{\lambda_g}{2\pi d} \tan\left(\frac{2\pi y_0}{\lambda_g}\right), \end{aligned} \quad (8.11)$$

where $x = k_2 d$. This equation is transcendental. The Taylor series for $\tan(x)$ contains infinite number of terms for correct representation. Such equations may have no roots or finite or even infinite number of roots. There exist no analytical means to solve such equations.

8.2.1 Graphical and numerical solution of the transcendental Eq.(8.11)

The roots of Eq.(8.11) needs to be localized by graphical methods. Later the accurate roots can be found out using the graphical root as the initial guess in a nonlinear root-finder. Once the roots are found, the dielectric constant of the solid can be evaluated as

$$\epsilon_d = \frac{k_{0d}^2}{k_0^2} = \frac{\lambda_0^2}{\lambda_{0d}^2} \quad (8.12)$$

where λ_0 is the wave length in free space and λ_{0d} is the wavelength in bulk dielectric

$$\begin{aligned} \epsilon_d &= \left[\frac{1}{\lambda_{gd}^2} + \frac{1}{\lambda_c^2} \right] \lambda_0^2 \\ &= \left[\left(\frac{x}{2\pi d} \right)^2 + \frac{1}{\lambda_c^2} \right] \lambda_0^2 \end{aligned} \quad (8.13)$$

since $x = k_2 d = 2\pi d / \lambda_{gd}$.

8.3 Experimental procedure

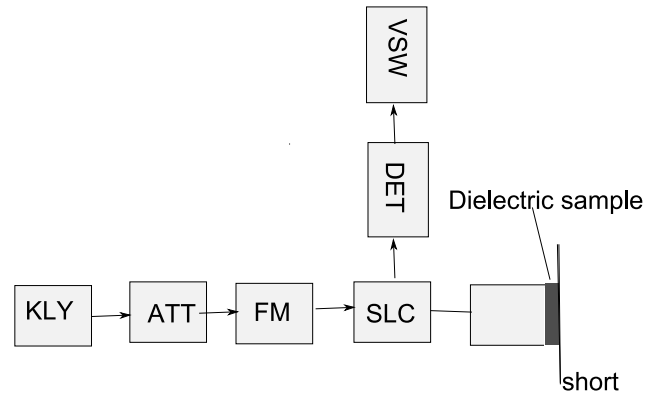


Figure 8.3: Experimental setup

1. Assemble the equipment as shown in the Fig.8.3.

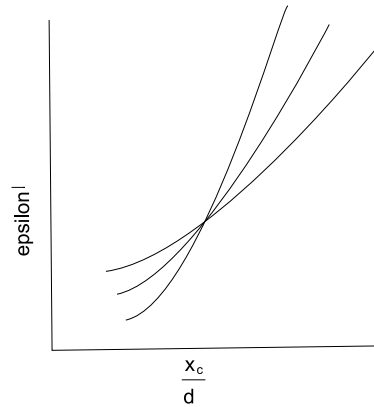


Figure 8.4: Graph

2. Energize the microwave and obtain the suitable power level in the power meter.
3. With no sample in the shorted wave guide, measure the position of the standing wave minima, starting from any reference plane. Compute the guide wavelength, the distance between successive minima is $\frac{\lambda_g}{2}$. The position of the first minima is taken as N_1 .
4. Use FM to measure the frequency of the excited wave and compute the free space wavelength ($\lambda_0 = \frac{c}{f}$). If frequency meter is not used compute it using the relation

$$\left(\frac{1}{\lambda_0}\right)^2 = \left(\frac{1}{\lambda_g}\right)^2 + \left(\frac{1}{\lambda_c}\right)^2 \quad (8.14)$$

where $\lambda_c = 2a$.

5. Insert the dielectric sample.
6. Measure the position of the standing wave voltage minima from the same reference plane. The position of the first minima is taken as N_2 .
7. Use Eq.8.3 to find y_0 by choosing the value n such that $0 < y_0 < \frac{\lambda_g}{2}$
8. Use Eq. 8.11 to find the value of $\frac{\tan x}{x}$. Now for this value find the first three possible solutions x_1, x_2 and x_3
9. Calculate ϵ'_i for each x_i . where $\epsilon'_i = \left[\left(\frac{x_i}{2\pi d}\right)^2 + \frac{1}{\lambda_c^2}\right]\lambda_0^2$
10. Plot ϵ' vs x_i/d . Plot it again for different sample length.
11. Find the correct ϵ' from the graph by taking the intersection. See fig:8.4.

Advantage of the method:

The method removes the possibility of the formation of air gaps in between the sample-waveguide wall and the sample shorting plate because the samples are compressed into pellets within the waveguide completely filling the waveguide cross section. Also removed are the ambiguities present in the selection of the phase factor (β). This method also removes the disadvantage encountered in the free space techniques such as the requirement for large sample surface area, the presence of unwanted reflections, diffraction effects and complicated experimental set-ups. This method is sufficient even for magnetic materials.

Appendix: MATLAB code for solving Eq.(8.11)

Eq.(8.11) is solved using the following code which has three segments, namely, *rootfind.m*, *input_tanx.m* and *tanxbyx.m*, which are given below. The routines are called sequentially just by running the main segment. It asks for an input where the value of a given by

$$a = -\frac{\lambda_g}{2\pi d} \tan\left(\frac{2\pi y_0}{\lambda_g}\right) \quad (8.15)$$

rootfind.m

```

1 clear all
2 home
3 global a d lamg;
4 prompt={'guide wavelength(lam_g)', 'position of minima(y_0)', 'length of the diel
5     def={'5', '0.5', '1'};
6     dlgTitle='Root Finder for tanx/x=a';
7     lineNo=1;
8
9     AddOpts.Resize='on';
10    AddOpts.WindowStyle='modal';
11    AddOpts.Interpreter='tex';
12
13    answer=inputdlg(prompt, dlgTitle, lineNo, def, AddOpts);
14    lamg=str2num(answer{1, :});
15    y0=str2num(answer{2, :});
16    d=str2num(answer{3, :});
17
18    a=(lamg/(2*pi*d))*tan(2*pi*y0/lamg);
19    xx=[];
20    yy=[];
21    for theta=0:2*360
22        x=theta*pi/180;

```

```

23     yy=[yy tand(theta)];
24     xx=[xx x];
25 end
26
27 plot(xx,yy)%ylim([-10 10])
28 hold on
29 plot(xx,xx*a)
30 for n=1:5
31     [x,y,button] = ginput(1);
32     input_tanx(x);
33 end

```

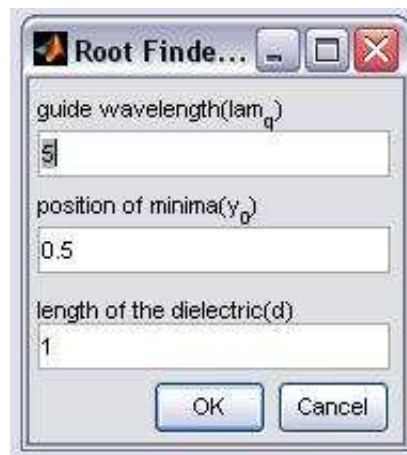


Figure 8.5: Input parameters

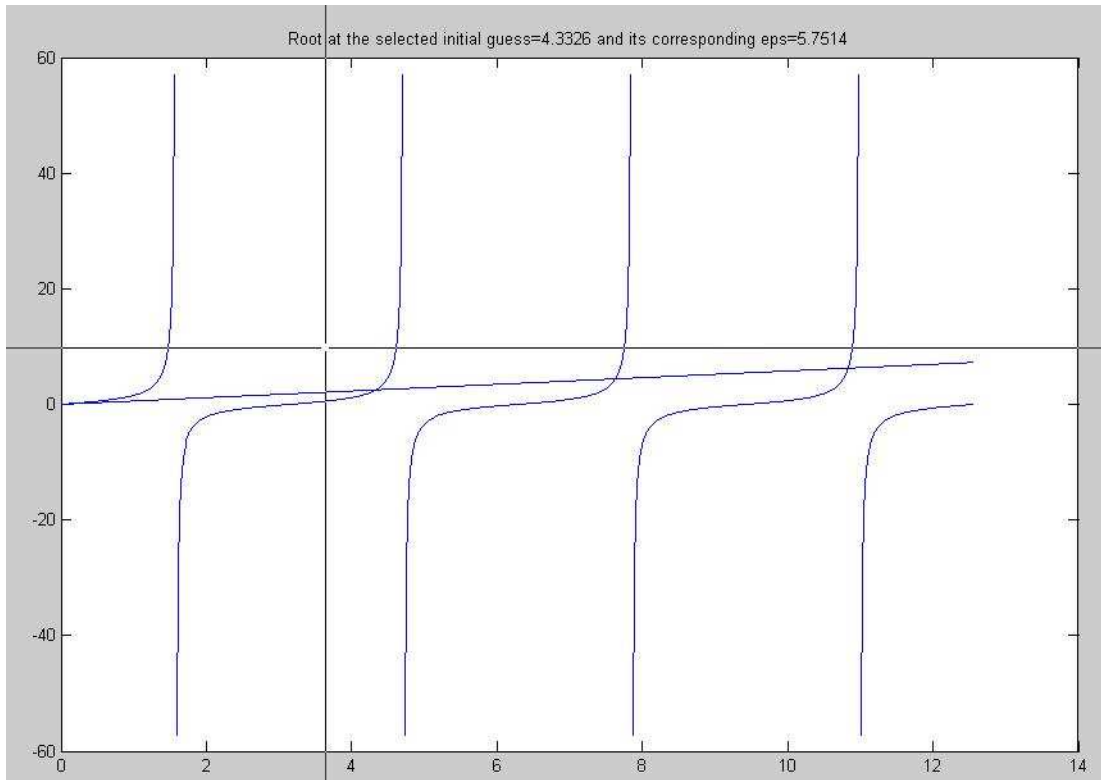
inputtanx.m

```

1 function input_tanx(x);
2 global d lamg;
3 lamc=2*2.2;
4 lam0=1/sqrt(1/lamg^2+1/lamc^2);
5 options=optimset('Display','off');
6 [x,f,exitflag]=fsolve(@tanxbyx,x,options);
7 eps=((x/(2*pi*d))^2+(1/lamc)^2)*lam0^2;
8 figure(1)
9 title(sprintf('Root at the selected initial guess=%0.4f and its corresponding eps=%0.

```

tanxbyx.m

Figure 8.6: $\tan x/x$

```
1 function f=tanxbyx(x);  
2 global a;  
3 f=tan(x)-a*x;
```

Chapter 9

Dielectric Constant of Liquids using Liquid Plunger

9.1 Theoretical background

The method proposed here uses a plunger for obtaining the standing wave profile in the sample, from which the attenuation constant (α) and phase factor (β) are calculated. A plunger was designed with its shorting plate fixed to one end of a brass rod, threaded with pitch. This rod passes through another cylindrical tube on which a main scale is calibrated. The plunger is useful as a movable shorting plate and for measuring the length of the sample in the waveguide up to an accuracy of 0.005 mm. It can also be used as a quarter waveguide.

Electromagnetic waves traveling through a lossy medium are characterized by the two complex parameters dielectric constant and permeability:

$$\epsilon = \epsilon' - j\epsilon'' \quad (9.1)$$

$$\mu = \mu' - j\mu'' \quad (9.2)$$

The amplitude varies exponentially as: $e^{j(\omega t - \gamma x)}$, where ω is the angular frequency and $\gamma = \alpha + i\beta$ is the complex propagation constant. As α is assumed always positive (to ensure loss in propagation), the waves are attenuated as they proceed forward:

$$e^{-\alpha x} e^{j(\omega t - \beta x)} \quad (9.3)$$

α is called the absorption coefficient and $\beta = \frac{\omega}{v}$ is the phase constant. From Maxwell's equations, one obtains for the phase velocity v in the medium:

$$v = c(\epsilon\mu)^{-\frac{1}{2}} \quad (9.4)$$

and for the propagation constant;

$$\gamma = \frac{j\omega}{c} \sqrt{\epsilon\mu} \quad (9.5)$$

For free space:

$$c = \frac{\omega}{k_0}, k_0 = \left(\frac{2\pi}{\lambda} \right). \quad (9.6)$$

In dielectric(Unbound medium):

$$v = \frac{\omega}{k_{0d}}, k_{0d} = \left(\frac{2\pi}{\lambda_{0d}} \right) + j\alpha. \quad (9.7)$$

$$c = \frac{1}{\sqrt{\mu_0\epsilon_0}}, v = \frac{c}{\sqrt{\mu_r\epsilon_r}} = \frac{1}{\mu\epsilon} \quad (9.8)$$

$$\frac{c^2}{v^2} = \epsilon_r = \frac{k_{0d}^2}{k_0^2} \quad (9.9)$$

$$\Rightarrow \frac{k_{0d}}{k_0} = \sqrt{\epsilon_r} \quad (9.10)$$

Low loss case

$$\alpha_d = 0 \rightarrow \epsilon^* = \epsilon = \frac{\lambda_0^2}{\lambda_{0d}^2} = \left[\frac{1}{\lambda_c^2} + \frac{1}{\lambda_{gd}^2} \right] \lambda_0^2 \quad (9.11)$$

Lossy dielectric

$$\alpha_d \neq 0 \rightarrow \epsilon_r = \frac{k_{0d}^2}{k_0^2} \quad (9.12)$$

$$\epsilon_r = \frac{\lambda_0^2}{4\pi^2} \cdot k_{0d}^2 = \frac{\lambda_0^2}{4\pi^2} \left(\frac{2\pi}{\lambda_{0d}} + j\alpha_d \right)^2 = \epsilon' + j\epsilon'' \quad (9.13)$$

9.2 Procedure

9.2.1 Lossless case

1. Assemble the equipment shown in the fig:9.1.
2. Energize the microwave and obtain the suitable power level in the power meter.
3. With no liquid in the cell measure the position of the standing wave minima, starting from any reference plane. Compute the guide wavelength, the distance between successive minima is $\frac{\lambda_g}{2}$.

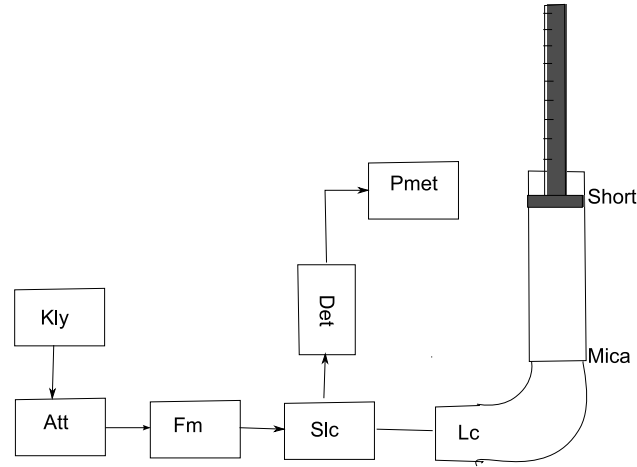


Figure 9.1: Experimental setup

4. Use frequency meter to determine the frequency of the excited wave and compute the free space wavelength($\lambda_0 = \frac{c}{f}$). If frequency meter is not used compute it using the relation

$$\left(\frac{1}{\lambda_0}\right)^2 = \left(\frac{1}{\lambda_g}\right)^2 + \left(\frac{1}{\lambda_c}\right)^2 \quad (9.14)$$

where $\lambda_c = 2a$.

5. Carefully detach the cell and fill it with a known volume of the liquid sample. And keep the short in its lowest position in the liquid column. Fix the detector at any desired position on the SLC.
6. Now readings should be taken corresponding to the different positions of the short in the liquid column(by increasing the height of the liquid column)
7. find λ_{gd} from the standing wave pattern Obtained from the above readings
8. find the dielectric constant(for lossless case) by using

$$\epsilon = \frac{\lambda_0^2}{\lambda_{0d}^2} \quad (9.15)$$

9.2.2 Lossy dielectric

1. Repeat the step discussed in the above section and plot the standing wave pattern. See fig9.3.

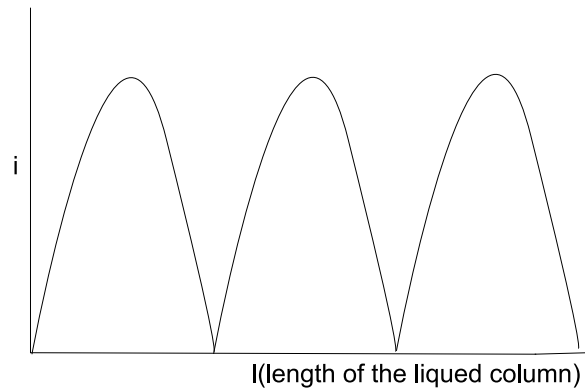


fig2: Lossless Liquid

Figure 9.2: lossless liquid

2. Find λ_{gd} from the distance between the peaks.
3. Plot a graph for $\ln\left[\frac{i_m}{I_c} - 1\right]$ versus the position of maxima m . Slope of this plot gives the value of $\lambda_{gd}\alpha_d$. Hence find α_d
4. Use eq9.12 to estimate the dielectric constant

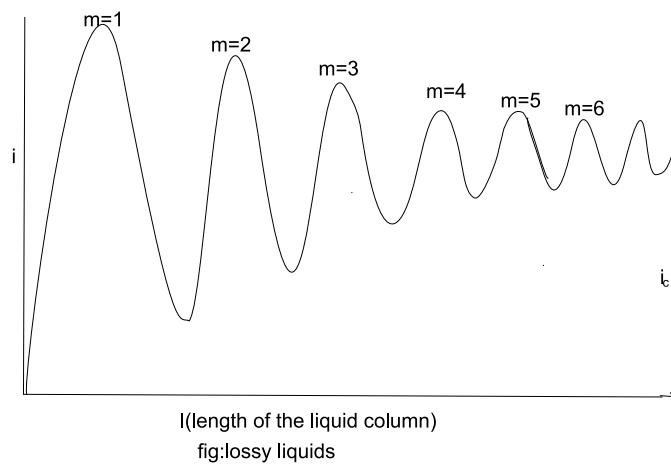


Figure 9.3: lossy liquid

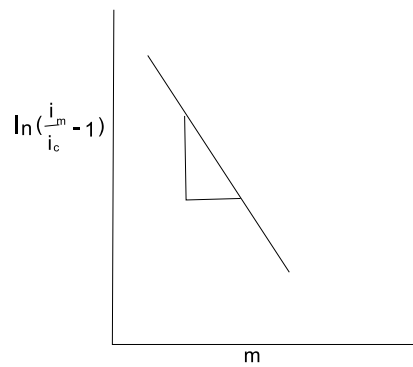


Fig4. $\ln\left(\frac{i}{i_c} - 1\right)$ Vs m

Figure 9.4: graph

Bibliography

- [1] Samuel Y. Liao, *Microwave Devices and Circuits*, (Prentice-Hall, New Delhi, 1995).
- [2] Simon Ramo, John R. Whinnery and Theodore Van Duzer, *Fields and Waves in Communication Electronics*, (John Wiley, Singapore, 2002).
- [3] E. V. Lebedev, *Microwave Techniques and Devices*, (Visshaya Schola, Moscow, 1970) volumes I and II (in Russian).
- [4] David M. Pozar, *Microwave Engineering*, (John Wiley, New York, 2004).

Acknowledgement

SDG acknowledges the help of two MTech CT students, especially of K Sarat for help in preparing the write-up. In the beginning they did not know Tex, nor Inkscape which were used extensively to prepare the text and the diagrams. Occasionally they wrote and tested the matlab codes which made data analysis simpler in many cases. Some theoretical analysis, like in Von Hippel's method was deduced from scratches by Sarat. Finally SDG would like to thank all the IV semester MSc students for their constant feedback on the typos/errors in the manuscript. It was indeed a pleasure to teach them and learn from them.